Universität Hamburg
DER FORSCHUNG | DER LEHRE | DER BILDUNG

Master Thesis

IoT-Based Solar Monitoring: Development of an Energy-Efficient System for Data Collection and Evaluation

Marvin Taube

marvin.taube@studium.uni-hamburg.de
Studiengang Master Informatik
Matr.-Nr. 7158355

Erstgutachter: Prof. Dr. Janick Edinger
Zweitgutachter: Dr. Philipp Kisters

Abgabe: 25.04.2025

Abstract

Renewable energies are a key component of a modern and sustainable society. Solar energy generation through photovoltaic (PV) panels is particularly relevant in urban environments because of the limited space available. In order to predict the potential performance of PV panels, solar potential maps such as the Solar Atlas Hamburg classify roofs according to their efficiency. However, as these datasets are derived from large-scale models, questions arise regarding their local accuracy and ability to capture distinctive features.

In this thesis, a cost-effective IoT-based sensor system was developed that enables the measurement of solar radiation and that can be used to validate existing solar potential maps, such as the Hamburg Solar Atlas. The aim was to verify and evaluate the accuracy of existing solar maps using real-world precision solar measurement data.

Several sensor modules were installed on various rooftop areas of the computer science Campus in Hamburg and operated over several weeks. The collected data was evaluated using a scenario-based approach and compared against the Solar Atlas. Particular emphasis was placed on detecting deviations and assessing the validity of the existing data at different locations.

The results show that while the Hamburger Solar Atlas provides reliable estimations in optimal areas, significant deviations can occur in suboptimal or shaded areas. In particular, significant deviations between the measurements and the existing data were found at locations with local particularities. The solar modules developed proved reliable and flexible for measuring solar energy, and the scenarios conducted contributed to the data-based evaluation of existing solar data sets.

Table of Contents

List of Figures

List of Tables

1 Introduction

This chapter begins by outlining the motivation behind this thesis. It then presents the objective by defining the research questions. At the end of the chapter, the general structure of this thesis is presented.

1.1 Motivation

Renewable energy has become indispensable in today's modern world. Many people want to contribute in using renewable energy, and the question arises of how best to do this. Solar energy is an interesting answer as it enables many individuals and companies to generate renewable energy on their balconies or company premises with the help of small solar systems, which are ideal for urban environments.

Although solar systems are becoming increasingly popular and available for companies and private individuals, many are still hesitant about installing a solar power plant on their roofs. Environmental sustainability is also an important factor in new constructions or renovations, and the extent to which solar power plants can be installed on buildings is usually examined. In order to check how much solar energy can be obtained from a roof, companies and cities have started to create solar data maps. However, these data maps are mostly snapshots, either measured on satellite images or, in the case of the city of Hamburg, with the Solar Atlas using a laser measurements, which is then enriched with various methods to make a statement about the potential solar energy on the roofs.

Since those data maps are usually only collected once as a snapshot and then on a large scale, much detailed information is lost. For example, something may have been built on the roof since the measurement for the map was made, or a neighboring house may have been built, which now casts a shadow on the roof. It is therefore interesting to examine how much such a solar dataset deviates from real-world measurement data and whether any systematic deviations can be observed.

1.2 Objective

To address the potential inconsistency and missing details information of large-scale data sets, this thesis deals with the first research question Q1 of how solar data sets can be evaluated and improved. Since there are several ways of evaluating data sets, this work is limited to missing detailed information described in the motivation. The goal is to

use precision solar data from roofs to evaluate and, if applicable, improve solar data sets based on more generalized collection methods.

> **Research Question Q1:**
> *How can precision solar data be used to evaluate and improve solar datasets that are based on more generalized collection methods?*

Since solar precision data is required, this work poses the second research question, Q2, to determine how precision solar data can be obtained.

> **Research Question Q2:**
> *How can precision solar data be collected to evaluate large-scale data sets?*

1.3 Structure

At the beginning of this thesis, Chapter 3 provides an overview of comparable work to illustrate the context in which this thesis is situated.

This is followed in Chapter 2 by the fundamental topics relevant to understanding this thesis and its context. First, the topic of IoT is briefly explained, followed by a basic introduction to solar energy.

Chapter 4 contains a requirements analysis to determine what requirements this thesis must meet to answer the research questions presented. Chapter 5 then presents the design that will be used to answer the research questions. First, the system design used to answer the first research Q1 question is discussed, followed by the design of a solar module to answer research question Q2.

Chapter 6 deals with the implementation of the presented designs. The various components of the design are discussed, and their implementation is described. The focus of this chapter is the development of the solar module used for precision solar data collection.

This is followed in Chapter 7 by the evaluation, in which various scenarios are described to evaluate the solar data set with precision solar values. This chapter also evaluates the requirements and the extent to which they have been met in this thesis.

In the last chapter, a summary of the results and a description of the implications of the results of this thesis is given. The limitations that arose during the thesis are then discussed, followed by an outlook on further topics.

2 Fundamentals

This chapter explains the fundamental topics that are necessary for understanding this thesis. First, the topic of IoT is introduced, and its significance for this thesis is explained. This is followed by a brief introduction to solar energy, describing what this energy is, how it works, and what is important for this thesis.

2.1 Internet of Things

The Internet of Things describes a concept that is an integral part of our modern world. IBM's definition describes the essence very well:

Definition 1 *The Internet of Things (IoT) refers to a network of physical devices, vehicles, appliances, and other physical objects that are embedded with sensors, software, and network connectivity, allowing them to collect and share data. - [ibm25]*

In the last few years, IoT has changed the world, and it is no longer possible to imagine it without it. IoT devices are everywhere, from the SmartHome temperature sensor to the laser calibration sensor in an industrial manufacturing complex or even just the heartbeat sensor in a smartwatch. All devices that collect data and make it available for analysis over the Internet can be accommodated in the concept of IoT [REC+15]. The Internet is only the means to an end of communication, to make the collected data of individual systems available and accessible.

IoT nowadays encompasses many areas and variations, specifying the concept for various domains. For example, the Industrial Internet of Things, which is discussed by [Sis+18], brings the topic of IoT into an industrial context and compares it to Industry 4.0. IoT devices and the concept can be found in almost every application area in the modern world. However, IoT is also a core concept for the modern smart city. The goal is to collect information about various areas using physical sensors. The aim is to connect all this information and make it available to the city and its residents to improve the city and life in it [Par25].

In the context of this thesis, the foundational aspects of IoT are applied through the design and implementation of a solar-powered sensor system tailored for precision solar data monitoring. The developed solar module aligns with IoT principles by operating autonomously, transmitting data wireless, and enabling data monitoring without manual supervision.

2.2 Solar Energy

When discussing solar energy, we refer to converting solar radiation into energy. The US Department of Energy [Res25] describes the process as transforming electromagnetic radiation into valuable forms of energy such as heat or electricity. However, the actual yield of electricity generation can vary significantly due to various factors such as geographical location, time of day, season, and local conditions [Res25].

In [Sto+10], three different units for measuring solar radiation that can hit a solar panel are described. The first form is direct normal irradiance (DNI), which describes the amount of sun radiation directed directly onto the panel. The second unit is diffuse horizontal irradiance (DHI). This is the reflected radiation, e.g., from the atmosphere or objects, which indirectly hits the solar panel. The third unit is the global horizontal irradiance (GHI), which is the total hemispherical irradiance. It can be calculated from the DHI and describes how much radiation hits a horizontal surface.

In [Bri25], three ways of obtaining solar energy are described. One is photovoltaic (PV) panels, typically mounted on rooftops. The other is concentrating solar-thermal power (CSP), a larger-scale system that relies on reflecting sunlight onto a central point to heat a medium that produces electricity. The third type is photo thermal, which generates electricity by using panels with a medium heated by the sun's rays. This thesis will deal with the first type, the PV panel, which will be further explained in the implementation.

To generate electricity with a solar panel, a load (consumer) must be connected to the panel to measure electricity directly. In [SP13], it is described how this consumer can be optimally calculated using maximum power point tracking. Since the PV panel generates different amounts of electricity at different solar radiation levels, optimizing the load for the respective situation is essential to obtaining as much electricity as possible from the PV panel. As an alternative to MPPT, fixed values can also be determined for a load. Although this does not result in optimal energy production, the power generated is still comparable, as then the only difference in electricity generation is the position of a panel itself.

3 Related Work

To provide an overview of relevant research work in the context of solar-related IoT measurement, Table 3.1 provides a structured tabular overview. The aim is to highlight similarities, differences, and this thesis's position in the field of research. The table summarizes the key features of the respective works and serves as a basis for the subsequent detailed discussion of individual approaches.

The selection of papers is mainly based on context and, technical relevance. Care was taken to ensure that solar measurement data was used wherever possible and that a technical approach was used to collect it. In addition, preference was given to papers no older than five years to provide the most up-to-date overview of the research.

The search focused specifically on work dealing with collecting solar-related data using IoT systems. Furthermore, work was selected that ideally included validation of the author's own data with reference data. In addition, work was sought that took a different technical approach to implementing the measurements to cover a broad spectrum of components used in developing the solar module.

Only works available to students with UHH access to scientific papers were considered for selection. This overview did not consider other work or resources that are only commercially available.

The columns in Table 3.1 have been chosen to show the technical implementation and the content contribution of each work. The first column of the table contains the reference to the respective work, which can be found in the bibliography.

The second column lists the respective units of measurement used in the various tasks to classify the sensors used. This makes it possible to distinguish which central measurement was relevant for the task. The table only describes the respective central measurements, other secondary measurements are not listed.

The geolocation is an important factor for recording solar energy, therefor the third column shows the location where the measurement was taken. Since some papers did not directly describe where the measurements were taken, the location of the primary author's institution was used.

Since a paper's objective significantly impacts the approach, the fourth column describes the objective of the respective paper.

A central point of this thesis is creating an IoT solar module intended to function as a sensor station. Since technical implementation is important, the work's approach on collection solar data is listed in the fifth column. The aim here is to provide an overview of possible technical implementations.

Table 3.1: Comparison of selected related works on IoT-based solar radiation measurement.

Source	**Measurments**	**Location**	**Objective**	**Technical Approach**	**Reference Data**
[Roc+21]	Global Irradiance	Urban (Brazil)	Real-time monitoring	ESP8266, Photodiode, MQTT	Yes, with INMET
[Tah+23]	Global Irradiance	Laboratory & Outside (Pakistan)	Development of an IoT pyranometer	ESP32, Peltier-Element	Yes, with Pyranometer
[Mel+21]	Solar radiation and PV output	Urban (Spain)	Monitoring of PV systems	Photodiodes, Cloud backend	Yes, with reference stations
[R+23]	Solar radiation, temperature, voltage, current	India	IoT-based measurement and monitoring system	ESP32, multiple sensors, cloud, app	No
[San+22]	PV power	Ecuador	Development of an IoT-based teaching system for PV monitoring	ESP32, cloud database	No
[Doz+23]	Solar radiation	Urban (Japan)	Development of a sensor with comparison to meteorological data	Microcontroller, MPPT, PV Panel	Yes, with meteorological data (JMA)
[RSY24]	PV power	indoor setting	Monitoring of photovoltaic systems	Arduino, solar panel, sensors	no
[HAI21]	PV power	Bangladesh	Real-time solar power monitoring system	ESP, INA219, PV Panel	no
This thesis	PV power	Germany (Urban)	Validation of urban solar maps	ESP32, INA219, PV Panel, self sufficient	yes, Hamburg Solar Atlas

The other central point of this thesis is evaluating the solar reference data set from the Solar Atlas Hamburg. The last column shows the respective reference data of the related works, if any were used for comparisons.

Most of the works from the overview in Table 3.1 either measure the solar radiation directly or derive the photovoltaic power from it. For example, while in [Roc+21] and [Tah+23] explicitly measure global radiation with specific photodiodes or Peltier-based sensors, studies such as [San+22], [RSY24], and [HAI21] focus more on the measurement of PV power data (e.g., voltage, current). Specific sensors are needed to provide accurate readings when measuring direct solar radiation. However, a simple solar panel is all that is needed to measure the electricity generated when measuring PV power. In addition, is the power generated by PV panels better suited for comparison because the data can be compared to existing solar installations.

The studies covered a broad spectrum, from rural applications to general test environments to highly urban scenarios. Since the context of the various studies sometimes only refers to developing a sensor module, the location is less relevant for this thesis. However, it is interesting to compare reference data in urban and rural contexts as differences in the available reference data become apparent.

Most works aim to develop a technically functional IoT system for measurement of solar data. However, the focus for the technical implementation varies. For example, in the work presented in [Tah+23], a focus is set on sensor development, while in [Roc+21], the focus was to integrate a real-time web-based visualization. This thesis aims not only to implement a functioning system but, in particular, at the validation and evaluation of public solar potential data (Solar Atlas Hamburg), which is not pursued in this form in any of the compared works.

Technically, many approaches are similar in using ESP32 or ESP8266, as in [Roc+21], [Tah+23], and [R+23] but some also use other controller like an Arduino in that was used in [RSY24]. The use of cloud platforms such as ThingSpeak or MQTT is also widespread. This thesis uses ESP32 with local data storage on an SD card and an optional uplink to a custom data platform. It was deliberately designed to be power-saving and fail-safe, focusing on modular expandability. In contrast to most other works, the evaluation, analysis, and presentation are performed manually and with custom services instead of using predefined cloud services.

Only a few studies perform a systematic comparison with existing data sources. In [Roc+21] INMET weather data were used for this purpose, [Tah+23] compares with a professional pyranometer, and [Doz+23] uses data from the Japan Meteorological Agency. The work [Mel+21] measures indirectly via PV energy availability, but comparison with external data is not a central objective. In [Mel+21] the data is compared indirectly, but it is not a central point. The works [RSY24], [HAI21], [R+23], and [San+22] do not perform any comparison at all. This thesis uses the raw data from the Solar Atlas Hamburg as a heat map and attempts to make statements about the accuracy of this reference data

using various scenarios.

4 Requirement Analysis

In this chapter, the research question Q1 posed in the objective of evaluating large-scale solar data sets is addressed, and requirements for this thesis are defined so that it can be successfully answered. In addition, requirements for collecting precision solar data are also defined, which should serve as a basis for answering the research question Q2 on the collection of precision solar data.

One approach to evaluating existing data sets is to collect new data. Since the primary use of solar data sets used in this thesis is the decision-making process regarding whether a solar power plant at a specific location is viable, it is essential to collect real-world data in specific locations to represent a potential solar power plant location. The new measurement data should be comparable to each other and to the large-scale gathered data sets to enable an evaluation of the collected data with the large-scale gathered data sets. To archive the comparison of the collected data and the data sets, the most important factors are the geographic location of the collected data and the comparability of the measurable units of the data. The measurement period also plays an important role, as a longer period makes the measurement data more accurate and less prone to errors.

To achieve accurate measurement results it is important to cover a sufficiently large period of time and have a sufficiently large number of different measuring points. Collecting those data points is essential to detecting and removing outliers and artifacts in the data that could affect the evaluation of the complete data set.

It is also important to compare the collected precision data with the large-scale data sets to gain a clearer understanding of the differences. Further, it is necessary to differentiate whether appearing deviations change with location changes or are constant over time. In addition, external influencing factors such as the weather should be included in the evaluation to ensure that both the large-scale gathered and the collected sensor data are influenced as little as possible.

Furthermore, the system should also be able to provide longer-term data to counteract the disadvantage of snapshot measurements. The following requirements for the overall system can be derived from the description above:

Requirement R1:
A large-scale solar data set is required, which can be used as a basis for evaluation.

Requirement R2:
It should be possible to determine precision solar data for specific geo positions.

Requirement R3:
The precision measurements should be comparable with each other and with the large-area data sets.

Requirement R4:
The measurement period must be long enough to collect enough data for an evaluation.

Requirement R5:
The measurement should use the same or comparable units in order to carry out the comparison and make meaningful statements.

Requirement R6:
Different measurement points must be considered to avoid local bias.

Requirement R7:
Faulty measurement data should not influence the evaluation.

Requirement R8:
It should be determined to what extent the measurement data deviates from the existing solar data sets and whether these deviations are local or global in terms of time or position.

Requirement R9:
External influencing factors should be taken into account in order to determine their impact.

As mentioned in 1.2, this thesis will also address the research question Q2 of how precision solar data can be collected to evaluate large-scale solar data sets. Therefore, requirements are also needed for the collection of precision solar data.

To collect precision solar data, the module must be able to capture solar radiation using a sensor and persist the collected data. Since solar energy is only collected outdoors, the module must also be able to withstand changing weather conditions. Solar power plants are usually installed on roofs, meaning the module should also be installed on roofs to ensure that the precision data acquisition is as accurate as possible. Access to roofs usually involves considerable effort, so the module should be self-sufficient for as long as possible to avoid maintenance costs.

To get as much data as possible in the limited timeframe of this thesis, the module should be easily scalable to collect data from many data points in parallel. As already described, the modules must be guaranteed to be robust against failures as they are installed outdoors. In addition, due to the positioning on roofs, there is usually no direct power connection available. Therefore, the module itself needs to work as self-sufficient and power saving as possible.

As this thesis is conducted in a university context, the multifunctional factor of precision data collection is essential to support as many research projects as possible. Therefore, the stations should also be able to allow other sensors. In addition, cost per module should be kept as low as possible to enable cost-effective data collection.

The following requirements for precision solar data acquisition can be derived from the description:

Requirement R10:
The recorded data must be persisted for later evaluation.

Requirement R11:
The solar module must be appropriately protected from different weather conditions.

Requirement R12:
The sensor system should be as robust as possible to run self-sufficient for an extended period of time.

Requirement R13:
The sensor system should be scalable to collect as much data as possible.

Requirement R14:
The sensor system should support collecting other sensor data besides the solar data for a multifunctional benefit.

Requirement R15:
The costs for a sensor system should be as low as possible.

5 Design

This chapter describes the design concept of this thesis using the requirements set out in Chapter 4. The system for evaluating large-scale solar data sets is presented first. This is followed by a more detailed presentation of the issue of collecting precision solar data and a description of a possible design for the solar sensor module. This chapter aims to establish the basic design that will be implemented and evaluated in the following chapters.

5.1 System Design Concept and Overview

As described in the requirements, this thesis will focus on collecting new precision solar data to compare it with the large-scale solar data sets to evaluate them. To achieve this goal, four components are needed, which are represented graphically in 5.1.

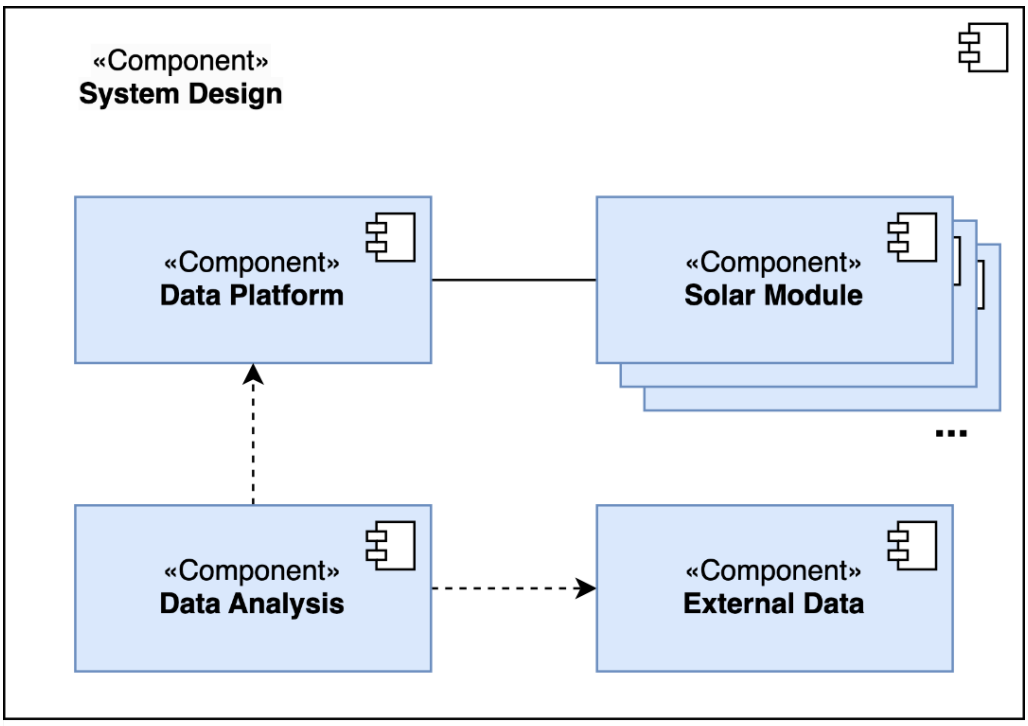

Figure 5.1: A component diagram illustrating the design of the developed system for evaluating solar reference data.

The first component is the solar module in the top right corner of the graphic. This module has the task of collecting the additional data required for the evaluation, which

fulfills the core requirement R2 that precision data can be collected. The design demands several identical modules to enable simultaneous data collection, which has the reason to collect as many sensor results as possible in the limited time of this thesis, which fulfills the requirement R4 and also the requirement R6 because multiple modules make it easier to collect same day data for different locations. Further, multiple modules also enforce the requirement R13 for scalability.

The solar module's design is strongly associated with the data platform component in the top left of the graphic. The data platform should serve as a central instance where the measurement data from other modules is collected and processed. Among other things, incorrect data should be cleaned up, corresponding to requirement R7, and the format should be adapted to compare the collected data with the large-scale data sets (R3, R5).

At the bottom right of the graphic is the External Data component which describes all external data but primarily fulfills the requirement R1 for a reference data set. The reference data set should be structured in such a way that solar data is available for the selected locations. The way in which the reference data set is collected is of secondary importance as long it is not based on precision data. Ideally, the data set should not be too outdated, as solar data in particular is susceptible to changes in the environment. This component also includes additional data, such as the external influencing factors enforced by requirement R7, which can for example be weather data.

The fourth component is the Data Analysis component at the bottom left of the graphic, which is an abstract component and describes the procedure for interpreting and evaluating the collected data. This component depends on the external data defined at the bottom right and the data platform at the top left, which provides the data for the analysis. This component aims to fulfill the analysis requirements R8 and R9.

5.2 Gathering Precision Data Concept

In addition to the requirements for the overall concept, requirements were also set for the precision data collection. To cover these, the solar module, which can also be seen as a component in 5.1, is shown in more detail in figure 5.2.

The solar module itself should consist of four components. The main component is the solar sensor at the top left of the graphic. This component represents the primary sensor used to collect solar power and the data needed for the evaluation. Thus, the module fulfills the requirement R2 for an option to collect solar data at a specific position.

The data storage component is located below the solar sensor at the bottom left of the figure. The data storage component is dependent on the additional sensor and solar component because its sole purpose is to preserve the collected data. Therefore, it fulfills the requirement R10 for persistent data storage.

The design also includes further sensors for the module, which are located in the Additional Sensors component at the top right. Even if the results of the additional sensors

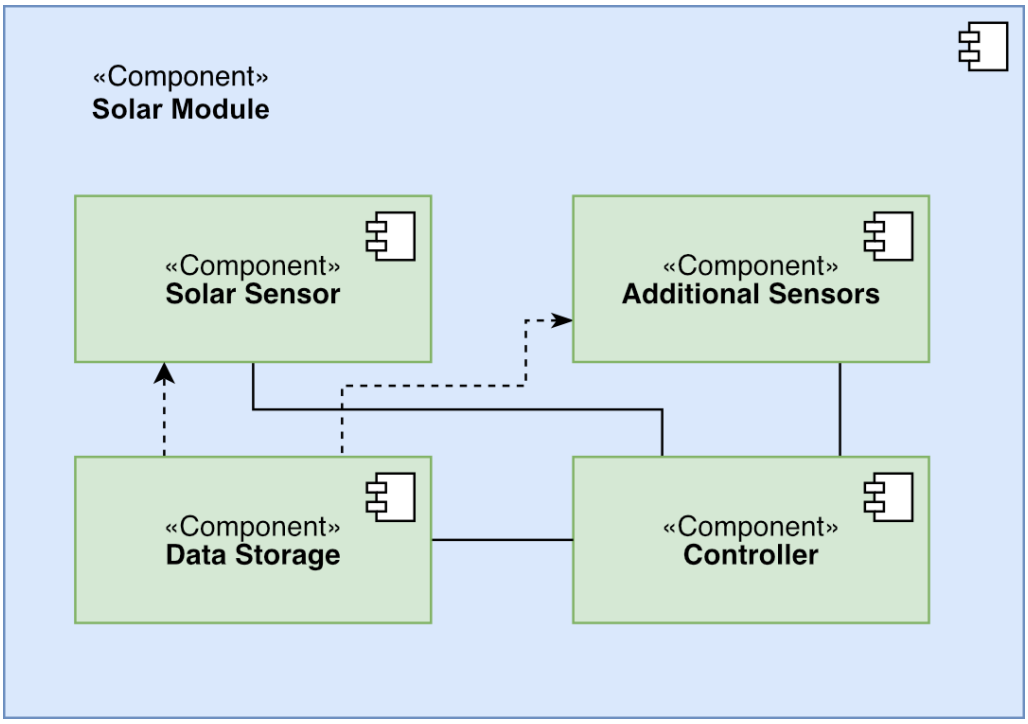

Figure 5.2: A component diagram illustrating the design of a solar module.

play only a secondary role in this thesis, further data collection is beneficial for comparing even more different data types. Further, can the modules be used again in the academic context to collect various sensor data, fulfilling the requirement R14.

All three components described above strongly depend on the control component at the bottom right of the figure. The control component describes the managing entity required by all components and sensors in the module. It is responsible for controller the module and making it an independent system. The controller should be able to supervise the connections between components and is responsible for the underlying workflow of the module.

5.3 Evaluation Concept

This thesis aims to evaluate existing solar data sets. To archive this, this section of the design concept describes how such an evaluation can be carried out.

One option for evaluating the solar data sets would be to use a scenario-based approach to test different setups successively. This approach evaluates different situations in stages, enabling a reactive approach when particular findings emerge.

An alternative to the scenario-based approach would be to evaluate long-term measurement data from different locations to gain insights that can then be used to evaluate the solar data set. Another option would be a simulation-based evaluation. This would involve attempting to replicate real environments under laboratory conditions or as a digital simulation so that no real measurements would need to be taken.

Another approach for evaluating the solar data set would be to distribute the solar modules to different people in the city to cover as many situations and locations as possible. Thus, large amounts of data could be collected that serve as the basis for the evaluation. Furthermore, crowdsourcing could be used here to obtain as much data as possible from other private sensors.

Due to the limited processing time, the scenario-based approach was chosen for this thesis. This has the advantage that it can be carried out in stages to react to the results and focus on the most interesting findings for the evaluation. For the long-term measurements, it would have been necessary to have collected data over a more extended period before this thesis was started. The simulation approach would also be challenging to implement if there are no real measurements to compare with the simulation. The crowdsourcing approach has the problem that significantly more modules are needed than a controlled scenarios would require. Furthermore, the results cannot be guaranteed to be comparable, as further problems cannot be ruled out if the modules are set up unsupervised.

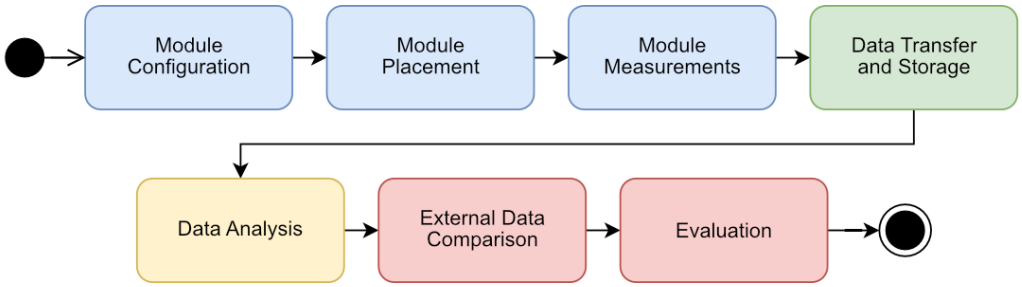

Figure 5.3: A activity diagram for displaying the design for executing one scenario for evaluating the solar reference data set.

The activity diagram in Figure 5.3 shows the concept for the sequence of a scenario for the evaluation. A scenario should consist of four sections indicated by four colors. The first section in the figure, marked in blue, contains three activities that should be performed sequentially, and describes the measurement period in a scenario. The first activity is the module configuration, in which the solar module should be configured to collect, store, and, if necessary, transmit solar data. The next activity is the placement of the modules. Different placements should be determined for the respective scenario, and the solar modules should be set up in the respective positions. The modules collect solar data for a specific period of time in the last activity of the blue section.

The second section is highlighted in green and contains only one activity. It describes how recorded data from all modules are collected and stored for subsequent analysis. The analysis happens in the third section, which is highlighted in yellow. It also contains only one activity and is responsible for preparing and analyzing the measured data. This activity aims to gain important insights from the collected data and process it so that it can be used for comparison and evaluation with reference data.

The fourth and final section is highlighted in red in the diagram. It describes the phase

in the scenario in which the measurement data is compared with the reference data to carry out the evaluation. The first activity in this section compares the measurement data with the collected solar data from the first section with existing external data. The external data includes the reference data set and other valuable resources for evaluation. The last activity is the actual evaluation and interpretation of the comparison which will help gain insights into the reference data set. Ideally, this activity also discusses possible setups for the following scenarios. The workflow presented here can then be repeated for each scenario to evaluate as many situations as possible in different scenarios.

6 Implementation

This chapter presents the implementation of the previously presented design. First, the solar module's development is discussed, focusing on implementing each component from the module design. A presentation of the implementation of the data platform and the analysis procedure follows this. Finally, the external data sets used in this thesis are presented.

6.1 The Solar Module

A specific module is needed to record the required solar precision data that can be then used for evaluation later on. As part of this thesis, a prototype module was developed that makes it possible to collect solar data at specific points at low cost. The module was designed based on the design presented in section 5.1 and is intended to fulfill the requirements for the collection of precision data established in the requirements in Chapter 4. The following subsections present the entire implementation of the solar module, including the implementation decisions of the individual components and their significance for fulfilling the design and the requirements.

The schematics of the finished module can be seen in figure 6.1 and it describes the individual components and how they are connected. For the schematics to be understood, it is necessary to describe the meaning the various symbols. The rectangles with a yellow background describe larger components, which are integrated into the module as ready-to-use components. This components are complete circuits that fulfill a certain function, and they can be bought as a complete module. The schematics red symbols represent analog hardware components, such as LEDs for visual feedback or resistors for regulating the current flow. These usually only fulfill one task and are less complex than the ready-to-use components, as they usually consist of only a single hardware component. The green lines are the connections of the individual components, but the components are only connected if a line connects them directly or if two green lines are connected, which can be recognized by a green dot on the connection point. The solar panel at the bottom left of the diagram and the battery at the top right should also be highlighted, as they count as external components for the module and are only marked with a connector symbol. The appendix provides an overview of the specific components, and the function of each component is described in more detail in the following subsections.

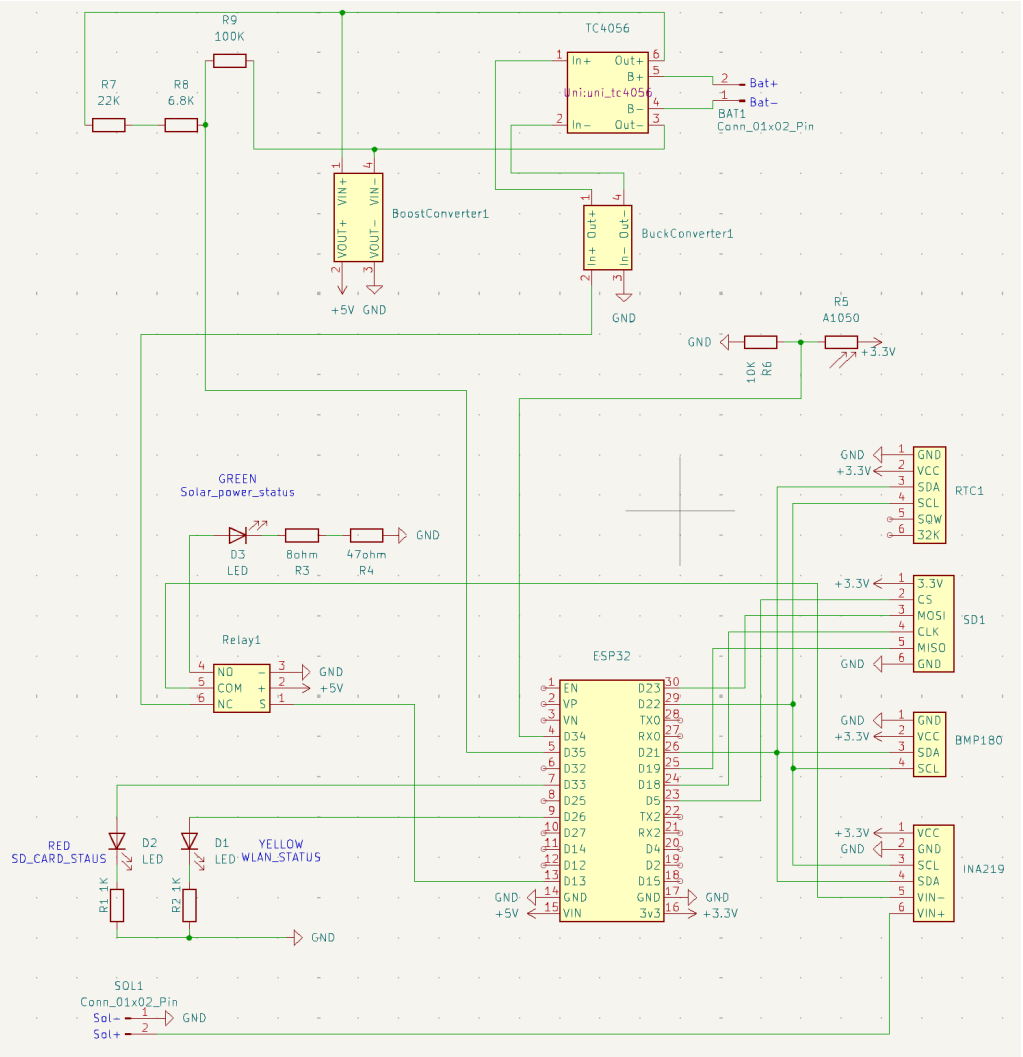

Figure 6.1: The entire circuit of the designed solar module.

6.1.1 Controller

A central processing unit is required to enable the module to collect and process data independently. The used controller can be seen in the lower center of the schematics graphic 6.1. The DEBO JT ESP32 microcontroller is used for the solar module developed in this thesis. This controller is a ready-made microcontroller from Joy-It based on the ESP32 chip developed by Espressif System. The ESP32 is a lightweight computing unit that requires a small amount of power but can still run more complex programs [esp25]. It has 4MB RAM and a 240MHz clock, sufficient for the intended use as a sensor platform controller. The advantage of the ESP modules is that they are equipped with an integrated Wi-Fi module. This means that the controller can also send live data to the intended data platform in the design, which benefits the requirement R12 of robustness. Furthermore, the ESP32 is also power efficient. With only 200mhw during Wi-Fi data transmission, the module is ideal control unit for as a self-sufficient solar monitor. Furthermore, it is possible to put the ESP32 into a deep sleep mode, in which it has limited

functions and can no longer send data via Wi-Fi, but it only consumes 2mWH of power, which is ideal considering requirement R12 for power-saving consumption. Since the ESP32 is a widely used microcontroller for IoT projects, these microcontrollers are also inexpensive to purchase, which is required according to requirement R15.

An alternative option for a microcontroller is an Arduino [Ard25]. These are less powerful in direct comparison with the ESP32 but are also more energy efficient on average. Arduinos also come without a Wi-Fi module as standard, making it more challenging to develop and live monitor the data transmission. In terms of price, the original Arduinos are significantly more expensive than the ESP32 modules. However, numerous copies can be bought for a comparable price to an ESP32 and offer the same range of functions as the original modules.

Another popular alternative is the Raspberry Pi or Raspberry Pi Pico [ras25]. The Raspberry Pi is more like a personal computer than a microcontroller and has far more computation power than an ESP32. However, because of its increased performance, it has a far greater power consumption and price than a microcontroller. Therefore, it would not be a good choice for a replacement in this implementation. A Raspberry Pi cloud can be used as a hub for multiple Solar Monitors to connect to in a more advanced setup. That would have the advantage that the Pi could collect and preprocess the collected data of multiple solar modules and would be a new redundancy layer to the design for temporary storage of the collected data.

The Raspberry Pi Pico is a scaled-down version of the original Pi and is comparable in price, performance, and power consumption to a microcontroller like Arduino or ESP32. The Pi Pico could be used as a replacement for the controller of the solar module, but it comes with the drawback that it does not contain a Wi-Fi module. Ultimately, the ESP32 was chosen because it best meets the requirements and already has the most features integrated in relation to its price.

Connections

The ESP32 microcontroller has several pins to which the other components are connected. Pins D21 and D22 on the right-hand side of the module are used for the I2C (Inter-Integrated Circuit) connection. I2C is a communication standard that allows multiple transmitters and receivers to use the same data line [Cam]. This is realized by giving each device its own I2C address with which messages can be sent to the correct receiver. For the implementation described here, this has the advantage that all components can be connected in series to the controller, making the implementation design simpler. Furthermore, it also has the advantage that additional sensors can be added to the current implementation design with little effort, given that they support the I2C protocol. In addition to I2C, the ESP32 also supports the SPI (serial peripheral interface) protocol, which is used by the SD card module in this implementation. The pins D23, D19, D18, and D5 on the microcontroller are used for this protocol. In contrast to I2C, SPI is supported by

fewer devices and requires more connections between masters and slaves [Dha]. In return, SPI offers a faster data connection and slightly lower power consumption. On the software side, there is almost no difference in which protocol is used as most standard libraries abstract both protocols and thus, the communication is implemented almost identically. However, the ESP32's support of both protocols has the advantage that a variety of additional components can be selected for respective tasks.

Further connections on the controller are those on the left-hand side of the module: D26, D33, D35, and D34. These connections are digital inputs or outputs that can output a PWM (Pulse Width Modulation) signal or read an electrical signal as an input. PWM describes the technique of changing an electrical signal in such a way that it can generate a variance in the voltage. With the microcontroller used here, input and output of signals in the range 0V - 3.3V is possible. The different voltages can be used, for example, to adjust the LED brightness or automatically switch electrical switches.

The pins at the bottom of the microcontroller GND, VIN, and 3V3 are the controller's power supply pins. VIN is the input, which can be up to 5V high. The 3v3 is an output pin that supplies power to 3.3V modules. GND is required to close the circuit in the entire module and all GND pins seen in the schematics 6.1 are connected via a GND plane to each other.

6.1.2 Solar Sensor

To fulfill requirement R2 that the module should be able to collect solar data, the module needs a solar panel to convert the solar radiation into energy that then can be measured. As described in the basics, different solar panels can be used for that purpose. The simple monocrystalline silicon solar panels are the cheapest and easiest to handle, making them ideal for this solar module. The solar panel used in this implementation is a 1W solar panel 100mm x 80mm, one of the smallest currently available on the market. This reduces the cost factor and thus meets requirement R15. In addition, the small form factor of those panels makes them easy to handle and the module small enough to be placed anywhere. A power of 1 watt is sufficient as the solar panel will mainly measure how much power is generated in relation to other positions and, therefore, does not need to be super powerful or efficient. Furthermore, the data collected from a small panel can easily be compared with data collected from other solar panels by scaling the factors accordingly. With an energy conversion rate of 15.5% of the panel's size and actual power generation, the collected data can be scaled to any other solar panel in any size, and therefore create comparable data. Moreover, the solar panel can also be used to generate electricity for the solar module, which is described in more detail in section 6.1.3.

Requirements for Measuring

As described in the basics 2.2, a solar panel needs a load, i.e., a consumer, to generate electricity. The ideal approach to implementing a load would be to install a component in

the solar module that can implement MPPT (Maximum Power Point Tracking) to adapt the load to the current solar power generation. However, these components are often more expensive than the cost this complete solar module without the MPPT controller, which conflicts with requirement R15, which states that costs should be kept as low as possible.

However, as the optimum load for a solar panel is a curve dependent on the voltage, an optimum load value can be determined for the average solar panel voltage. In this context, load or consumer describes nothing other than how much electricity must be consumed so that the solar panel can generate electricity as efficiently as possible.

The simplest form of a constant load is a resistor, which converts electricity into heat when current flows through it. It is essential that the resistors can withstand enough power before they break down. To determine what resistance value is required and what power the resistor must be able to withstand, the following calculation 6.1 can be made.

$$R = \frac{V_t}{A_t} = \frac{5,5V}{0,1A} = 55\Omega \tag{6.1}$$

In calculation 6.1, the typical generated voltage V_t of the solar panel is divided by the typical generated current A_t of the solar module to calculate the constant resistance for the solar panel using Ohm's law to approximate the optimal load. This solar module uses two safety resistors, with values of 8 Ohm and 47 Ohm, in series to achieve a resistor value of 55. The safety resistors are coated with a heat-resistant layer, making them safe for power values of up to 2.5W, which is far more than the 1W solar panel can generate.

The resistors used can be seen in the center-left of the schematics overview 6.1. In addition to the resistors, a green LED can be seen there, fulfilling two functions. Firstly, it serves as a status indicator to show that the solar panel is generating power. Secondly, an LED (Light-Emitting Diode) is nothing more than a diode that only allows current to flow in one direction, thus ensuring that electricity cannot flow backwards in the circuit.

To prevent the constant load value from being falsified by other consumers in the circuit, it is essential to ensure that the solar panel is not connected to any additional loads during the measurement, which also affects the module itself. This means the solar module requires a separate power supply that is seperated from the solar panel so as not to falsify the measurements.

If a larger solar panel or one with more power were chosen for the implementation, only the calculations for determining the optimum load would have to be adjusted to record comparable data, making this setup ideal for comparing modules of different designs. However, using only identical modules keeps the effort as low as possible.

Measuring Solar Radiation

Most data sets have their information on power generation given in watt-hours per area. This means that the solar module must determine how many watt-hours are generated

at a particular position over a specific period of time with the selected solar panel.

This solar module uses an INA219 sensor module to measure both amperage and voltage, which are required to calculate watts, as accurately as possible. The sensor communicates with the microcontroller via I2C and can be set to a detailed mode to detect even the most minor changes in voltage and current.

The INA219 supports various sensor modes. The standard case is that the sensor only measures how much current is currently being generated at the measuring point. The alternative mode is that an average is measured over a longer period of time, which is then transmitted at the time of measurement. It may seem that the alternative measurement mode is better suited for obtaining continuous data, but this would require the solar panel to be permanently connected to a constant load. However, since the solar panel is also used to charge the battery, the power generation cannot be measured all the time, and therefore the normal measurement mode must be used. How exactly the solar panel is used as a sensor and as a charger is described in the following sections.

Separate modules can also be used to record the solar panel's voltage and current as an alternative to the INA219. In the design of [RSY24], a dedicated sensor is used for the amperage and for voltage. A significant disadvantage of the modules used in that work is the resolution rate of the sensors, which are not high enough to sens minor changes like those in a solar panel under suboptimal conditions. Since the solar panel generates electricity very variably, precise measurements are relevant depending on the current solar radiation.

6.1.3 Power System

To meet the R12 requirement, the solar module must be powered over a more extended period, even without a power outlet. As already described in the design, the solar modules are installed on roofs where a direct power connection is usually impossible. To decide what battery capacity is required for the module, Table 6.1 shows the power consumption of the used components.

The microcontroller has the highest power consumption is during data transmission. However, this value can be reduced by limiting the transmission periods and setting the controller to deep sleep mode. The comparison of the power consumption can be seen in the right-hand column in Table 6.1.

A processing interval of 60 seconds is selected to minimize power consumption. The module is in transmit mode for 6 seconds, carries out all sensor measurements, persists the data, and transmits it to the data platform if Wi-Fi is available. For the remaining 54 seconds, the controller is in deep sleep mode and only partially supplies the other components with power. Using the current values of the components and the active times of the controller, it is possible to calculate how high the module's power consumption is,

Component	Active State	Deep sleep / Inactive
ESP32 Microcontroller	$\sim$ 150mA	$\sim$ 1.5mA
Relay	$\sim$ 60 mA	0 mA
INA219 & BMP180	$\sim$ 3.3 mA	$\sim$ 0.03 mA
SD Card Module	$\sim$ 30 mA*	$\sim$ 3 mA
RTC	$\sim$ 5 mA	$\sim$ 5 mA
Buck / Boost Converter	$\sim$ 12 mA	$\sim$ 12 mA
Rest Components	$\sim$ 15 mA	$\sim$ 10 mA

Table 6.1: Power consumption of components in the solar module.

which can be seen in the equation (6.2).

$$\begin{aligned} P &= \sum C_I \cdot \frac{54s}{60s} + \sum C_A \cdot \frac{6s}{60s} \\ P &= 31.53mA \cdot 0.9 + 275,3mA \cdot 0.1 \\ P &= 55.91mA \end{aligned} \tag{6.2}$$

To calculate the power consumption of the whole solar module 6.2, sums are calculated from the power consumption values of the individual components from Table 6.1. A distinction is made between the active C_A and inactive C_I states (deep sleep) in which significantly less power is consumed. The factors of the individual values result from the selected interval in which the solar module is active. Scaling to the hour is trivial if an active interval of 6 seconds is used, as in this implementation.

This thesis uses a lithium-ion battery with 6000mAh to achieve a compromise between the requirement R15 for the lowest possible costs and the requirement R12 for a self-sufficient behavior. With this battery size, the solar module with a power consumption of 55.91mA, can be operated for 107.3 hours (4.5 days) without an external power supply.

Alternatively, a larger battery could have been used to increase the module's runtime or a smaller one to reduce the costs per module. Another option would have been to use typical AA or AAA batteries, but this would have further limited the uptime and prevented the possibility of recharging the module.

Since lithium-ion batteries are not safe to handle without protection, a charge control chip that monitors the battery and, if necessary, interrupts the power supply if the battery is too full or too empty is necessary to protect it and the entire system. The solar module's charge controller is the TC4056, which can be integrated into the module and provides an integrated charge protection circuit. An additional advantage is that the charge controller board comes directly with a micro USB port which makes it possible to change the battery directly, so that a dedicated charging station is not needed to charge empty batteries. Alternatively, other charge controllers, such as the TP5100, could be used, but the TP5100 for example would require a higher input voltage.

Figure 6.2, shows a section that represents the power system of the complete schematic

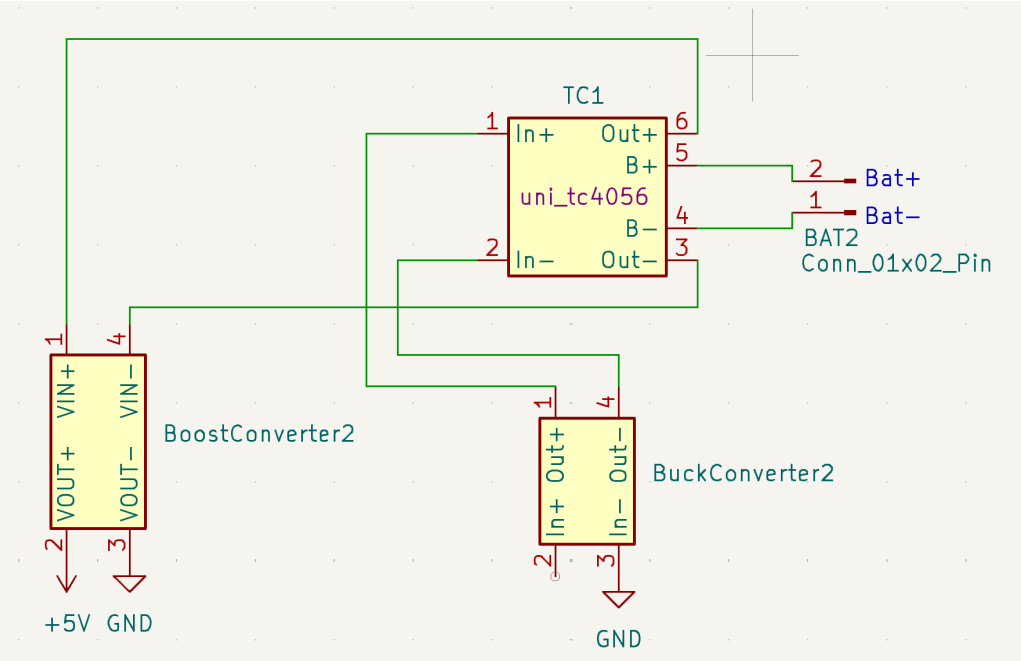

Figure 6.2: A circute section highlighting the power circuitry of the implemented solar module.

seen in figure 6.1. The connection between the battery and the TC4056 charge controller can be seen on the right of the site of the figure. The output from the charge controller on the right is then connected to a boost converter, which can be seen on the left in the power schematics 6.2. A boost converter is a component that can efficiently increase an input voltage. Here the output voltage from the TC4056 is efficiently scaled up from 4.2V to 5V and sent directly to the microcontroller. This is necessary because some components in the circuit presented, such as the relay and the microcontroller, require 5V directly. The microcontroller can also be supplied with 3.3V, but a 5V supply ensures that the controller has enough power to power itself and all other components that are connected to it. The components that require 3.3V are then directly supplied from the microcontroller. A buck converter can also be seen at the bottom right of figure 6.2. The buck converter takes on the opposite role of a boost converter and efficiently scales down a voltage. With this specific solar module, any input voltage is scaled down to 5V in the boost converter and then fed directly to the charge controller. This is necessary because the charge controller tolerates a maximum input voltage of 5.5V until it breaks, but the solar panel supplies at max 6.4V.

The detail power view does not show that the buck converter's input is connected to a relay. A relay is an electromechanical switch that can be toggled via an electrical signal. Since the requirement R12 is to be self-sufficient and there is already a solar panel for the sensor data, it makes sense to use this solar panel to charge the module's battery. However, the section above already explains that a constant load is required to obtain comparable sensor data. Connecting the solar panel to the circuit of the solar module would,

therefore, falsify the measurement data. To prevent this, the solar panel is connected to the relay input. This can be seen in 6.1 where Sol+ first goes into the INA219 for the measurement and then into the relay. In the normal state, when the relay has no power, this connects the solar panel to the buck converter and thus to the charge controller and then to the battery to charge it. When the sensor interval occurs, the relay receives a signal from the microcontroller. It disconnects the solar panel from the charging circuit and connects it to the safety resistor for the constant load so that the measurement can occur. After the measurement, the relay switches back, and the solar panel can be used to generate power for the battery.

A simple calculation can be done to determine the effect that connecting the solar panel at non-sensor intervals has on the runtime of the solar panel. Assuming the solar panel generates an average of 300mWh and is connected for just under 6 hours, 1800mW of electricity can be generated daily, increasing the module's runtime.

6.1.4 Data Storage

The next component required by the design for the solar module is data storage. It should be possible to persist the collected data for analysis and evaluation. The solar module fulfills this in two ways.

First, an SD card reader containing a 4 GB micro SD card is installed in the solar module. All sensor data from all measurement intervals are stored on this card, which fulfills the R10 requirement.

Using SD cards with less storage space would have been sufficient, but 4GB is already one of the smallest capacities currently available. And since these SD cards are standard sized, they are also sometimes cheaper than SD cards with lower capacities.

Additionally, the microcontroller's Wi-Fi connection is also used to transmit the data directly to the data platform. If a Wi-Fi connection can be established at the start of the sensor interval, the data is transmitted to the data platform for external storage and in additionally on the SD card for local storage.

6.1.5 Additional Sensors and Components

The design also includes a component in the solar module for additional sensors. This is due to requirement R14, which requires the solar module to be used for other measurements.

In the version developed in this thesis, an additional temperature and pressure sensor was integrated as a proof of concept. The only conditions for the integration were cost efficiency and the communication interface. Since it is an additional sensor that is not directly needed to answer the research question, just a simple BME180 sensor is installed for the temperature recordings. This is one of the most cost-effective temperature sensors that support the I2C interface and can be easily integrated into the existing circuit.

The solar module also contains a light sensor. In contrast to the solar panel, this cannot make statements about the possible electricity production but rather about the ambient light, i.e., the brightness that hits the module. For example, to make statements about light pollution at night.

Alternatively, any sensor supporting one of the supported communication protocols could be integrated into the solar module. In addition, various digital pins on the ESP32 are still free and could be used to connect other sensors to the module.

Another component connected to the solar module is a realtime clock (RTC). This ensures that the time is retained when the module is switched off. Suppose the microcontroller runs out of power and is entirely offline. In that case, it will stop counting the time and, when restarted, have the wrong timestamps for the data entries, assuming there is no Wi-Fi connection for synchronization.

The RTC is connected on the right in the overall schematics to the ESP32 via I2C. The RTC module can track the time correctly even when it is offline because a capacitor battery is attached to it, continuing to supply it with power. If the solar module is supplied with power, the battery power is not used for the RTC, which increases the battery life of the RTC and, therefore, rarely needs to be replaced.

Three resistors can be seen at the top left of the schematics overview. These resistors are intended to function as a voltage divider to read out the current status of the battery. The voltage divider is necessary because the ESP32's analog inputs can only support a current voltage of 0V—3.3V, while the battery's voltage limit is 2.2V—4.2V. The three resistors with the described values scale the voltage accordingly so that the ESP32 can interpret them. This would enable the ESP32 to read out the battery's current status and thus monitor maintenance periods, for example, as the batteries can be replaced more efficiently. Due to time constraints, the PCB is designed to accommodate a voltage divider for the solar module, although the resistors are not included in the final assembly.

Alternatively, any other sensor or component can be connected to the solar module. However, it should be ensured that the selected microcontroller has sufficient pins to connect all components and enough computing power to process all data efficiently. Furthermore, installing more sensors also means a higher power consumption of the solar module. Proper caution should be exercised when choosing a smaller solar panel or battery to ensure the self-sufficiency requirement is not compromised.

6.1.6 Production Ready Module

Since this thesis aims to design several modules that can be used even after the completion of this thesis, some components are still not directly listed in the design but are needed to fulfill some requirements.

First, requirement R11 demands that the developed solar module be weatherproof so that it can be set up outside for a longer period.

As shown in figure 6.3, the finished module is integrated into a box so that the elec-

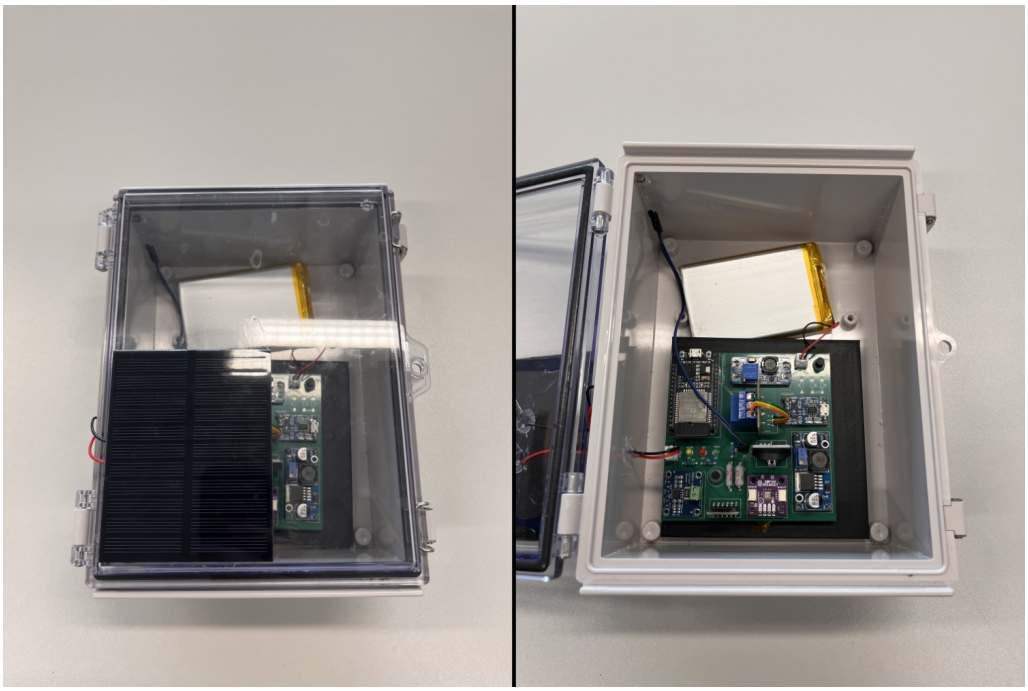

Figure 6.3: The developed solar module with weatherproof box and custom PCB.

tronics can withstand different weather conditions. The box is IP67 qualified and can be mounted outside on roofs for extended period of time. As can also be seen in figure 6.3, the solar panel is attached to the outside of the module. This is because the material restricts solar radiation even if the lid is translucent.

As can also be seen in the image of the solar module, a separate PCB was designed for it. This mainly fulfills the requirement R12 for robustness and R13 for scalability, and R15 for price reduction. A custom PCB increases the module's robustness, as the electrical connections of the individual components are more stable than if a breadboard and cable connectors were used. The requirements R13 and R15 are fulfilled as printing several PCBs is much cheaper than buying cables for several modules to connect the individual components. At lower quantities, a PCB costs almost half as much as the required cables to connect all modules, and at higher scales, the difference is even more significant.

As mentioned in some of the sections above or as seen in circuit 6.1 or in the finished solar module 6.3, three LEDs are also attached to the module. The LEDs serve as a status indicator for the solar module and are intended to facilitate module maintenance. The red LED is a status indicator to show whether there is a problem with the SD card. If it lights up when the solar module is started, the MicroSD card cannot be read or written to and must be replaced. The yellow LED also lights up when the module starts up while trying to connect with the Wi-Fi. If it lights up for 10 seconds, the connection to the stored Wi-Fi network cannot be established. The green LED, on the other hand, is a positive feedback signal. This only lights up when the solar module is in the sensor interval, and the solar panel generates power.

LCDs, which are relatively inexpensive and can also be connected to the microcontroller via I2C, and are a frequently used alternative for status displays. A possible implementation of a display on a solar monitoring system can be seen, in [Kat+18], where it is used to display realtime information of the module. The significant disadvantage of displays, is that they require more power, which would limit the runtime of the solar module, which speaks against requirement R12 that the modules should be able to function as self-sufficiently and independently as possible for a long time.

6.1.7 Process

Since the previous sections discussed the individual components of the solar module, this section describes the process for performing a solar measurement in the finished solar module.

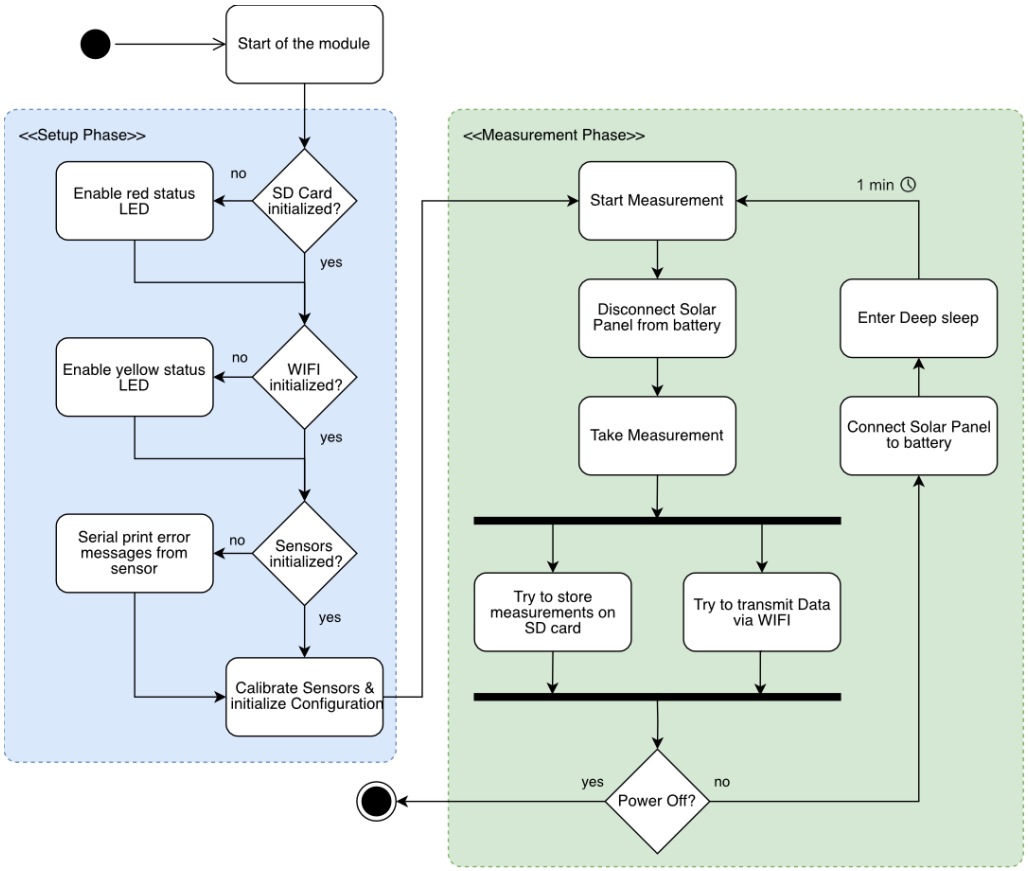

Figure 6.4: An activity diagram illustrating the process in a solar module.

The activity diagram in Figure 6.4 visually illustrates the workflow of the solar module from power-up to power-down. Generally, the solar module process can be divided into two phases and three areas. The first area does not belong to any phase of the module, and can be identified with the area with no background color. It describes the beginning and end of the process, which must be carried out manually. This area contains only one action which is the start of the module which happens when it is powered on.

The second area and the first phase of the process is the module's setup phase, which takes place immediately after the module is started. This setup phase is marked with a blue background in the figure 6.4. In this phase, the system checks whether the essential components have been initialized correctly. First, it checks whether local storage is available, and if not, a red status LED is activated. Next, it checks whether the module can establish a Wi-Fi connection. If this is not possible, a yellow status LED is activated. The initialization of all sensors follows this. If there are any errors during initialization, they are output via the serial interface. Once all components have been initialized, the sensors are calibrated, and if a configuration is available, it is loaded, and the system moves on to the second phase.

The second phase, and thus the third area, is marked with a green background and describes the measurement phase. The phase starts when the measurement is started. To do this, the solar panel is first disconnected from the battery to prevent the main circuit from influencing the measurement. The actual measurement of the INA219 takes place. In this segment, all measurements from any additional sensors are also carried out. The sensor data is then stored locally if local storage is available, and if a Wi-Fi connection has been established, it is transmitted in parallel to the platform. If the module is then powered down, the process is interrupted here and ends until the module is switched on again. If the module is still powered up, the solar panel is reconnected to the battery, and the module puts itself into a deep sleep mode, which lasts for approximately one minute until the measurement is performed again.

6.2 Data Platform

In the design, the data platform should collect and store data from the various modules. The aim is to create a possibility to persist the data in a structured way and to make it available for later analysis. It can also be used to monitor live information about individual modules if an appropriate presentation of the data is implemented. The data platform should not perform any complex operations itself and, therefore, focuses more on robustness, availability, and simple integration.

NUXT [Nux16] is used for the data platform in this implementation. Nuxt is a Node-based Javascript framework that allows the writing of server-side code with VueJS [You14]. Nuxt makes it extremely easy to create a functioning API in short time using file routing and supports all standard Node packages for database integration. The developed data platform provides only one API endpoint for storing measurement data, which the modules can access directly via HTTP.

A data store is needed as part of the data platform to store data persistently. This implementation uses a MongoDB [Mon25] as a data store. It is a NoSQL database that stores JSON objects directly in a database table. In the limited time frame of this thesis, the goal was to start collecting solar data from the modules as early as possible to obtain

as much data as possible for the evaluation. Therefore, the data platform and the data storage were required to be as flexible as possible and adapted quickly if the format or structure changed. Furthermore, the NoSQL approach has the advantage that all data is initially stored, even if the data has a different structure. This results that no data is lost, even on misconfiguration of the data platform.

An Express [Fou25] instance is set up to retrieve the data, and enables direct access to MongoDB. This has the advantage that no separate interfaces are required to query the data. The Express instance allows the stored measurement data to be exported directly as CSV or JSON, which is supported by most data analysis programs and is sufficient for the scope of this thesis.

6.3 Analysis

Another component of the system design is analyzing the collected data and the associated in-depth evaluation of a large-scale solar data set. Hamburg's Solar Atlas, which is described in detail in section 6.4.1, will serve as the evaluation basis for the analysis.

As outlined in the design, the idea is to implement a scenario-based approach. This is done by analyzing specific situations from the reference data set. For each scenario, a specific property of the data set is checked and evaluated using the precision solar data.

The collected precision data is taken directly from the data storage for each analysis and, if necessary, adjusted in the format. The presentation of the collected data is primarily visualized using graphs that represent the power production over a certain period. This is because the comparative data from the Solar Atlas Hamburg is not recorded precisely and not available with absolute values, and can therefore not be compared to absolute values. Hence, a mathematical comparison is only possible to a limited extent. The evaluation should then be carried out using relative relationships between the precision data and the data in the dataset to determine whether corresponding findings can be obtained from the comparison.

Python libraries such as matplotlib [tea12] and numpy [tea25], which have established themselves as the standard for data analysis, are used to analyze the collected data and create the graphics. The data is exported from the corresponding tables in the data storage as CSV and analyzed locally. Since the evaluation is scenario-based, data was collected for most scenarios for two weeks, with up to four modules.

As the data is available in a NoSQL database, any data analysis tool that can connect directly to the database, interpret the JSON file format, or support data import as CSV can be used as an alternative.

6.4 External Data

External data is required to as an evaluation basis for the solar data collected from the modules. The basis for comparison in this thesis is the Hamburg Solar Atlas, presented in the following.

Furthermore, other external data is also required to put the measured solar data into the proper context. This section also briefly presents data from the Deutscher Wetter Dienst and the Solcast API for this purpose.

6.4.1 Hamburg Solar Atlas

To answer the research question Q1 and fulfill requirement R1, a large-scale solar data set is required that can serve as the basis for evaluating the data. The Hamburg Solar Atlas [Ham24], which can be seen in figure 6.5 is primarily used for this purpose in this thesis.

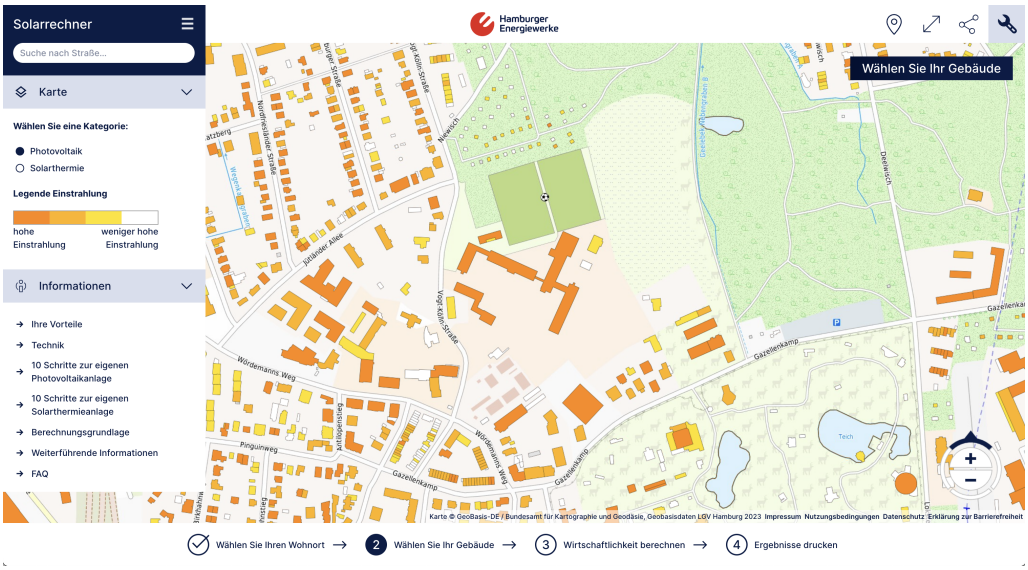

Figure 6.5: Web view of the Solar Atlas Hamburg for the computer science campus. [Ene25]

The State Office for Geoinformation and Surveying of the City of Hamburg (LGV) made this Hamburg Solar Atlas available to the residents of Hamburg. In addition, the Geoportal Hamburg [LGV25] provides an interactive map to display solar information from the entire roofs of the city.

The data set was created to allow the city's residents to interactively determine the extent to which a solar installation on their roof would be financially worthwhile. In addition to the interactive map with various views, the city provides the roof for some roof in CSV files.

THe basis for this data set was only collected once in 2018, so it is an excellent basis for evaluating whether the data collected over a large area is up-to-date and correct. The

data was measured by laser detection by airplane and has not been updated since.

In addition to the publicly available data, it is interesting to see how data set behaves,for individual roof with lokal anomalies. The irradiation view is interesting, as the publicly available CSV datasets only contain information on certain entire roofs or areas on roofs instead of points. On request, the City of Hamburg provided the original heat maps for this thesis.

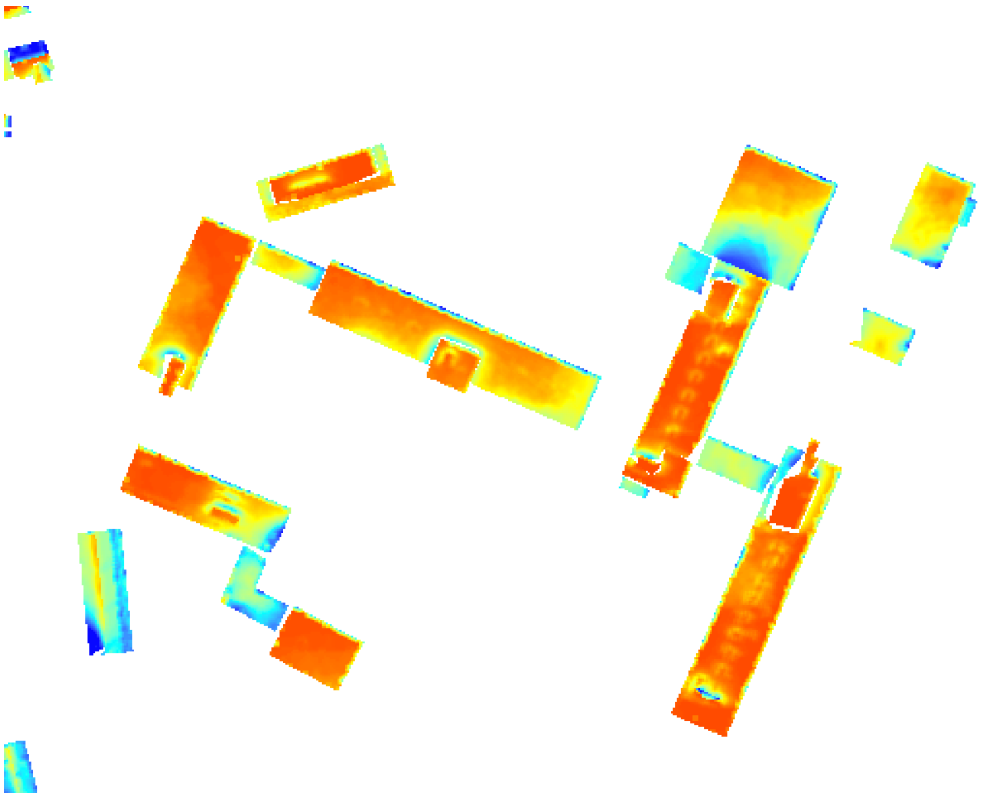

Figure 6.6: Heat map visualization of raw data from the Solar Atlas of the Informatikum in Stellingen.

Figure 6.6 shows our computer science faculty's original heat map data. What is easy to recognize is that there were different strengths of irradiation on the roofs. The city of Hamburg provided no information about the exact measured values for the color points. However, this is not a problem, as the measured solar precision values can be relatively compared to the data set to evaluate the data.

6.4.2 Deutscher Wetterdienst

Regardless of the data set to be evaluated, it makes sense to enrich the collected precision data with additional information to improve it further. The Deutscher Wetter Dienst [dwd25] operates many weather stations throughout Germany, collecting temperature, wind, solar, and precipitation information. The various stations are not identical in construction and sometimes differ in capacity. One weather station is at Hamburg Airport, near the computer science campus.

An interesting metric that is collected there is the actual hours of sunshine. This value describes how much sunlight the station has received during the day. As it is difficult to directly correlate the weather or individual clouds, with the measurement results, the metric of hours of sunshine offers a good opportunity to make a statement about the performance of the solar modules.

6.4.3 Solcast API

Another interface that enriches the data further is the Solcast API [sol25]. This API provides additional solar-based information, such as DHI, GTI, GHI, and DNI, as well as weather information, such as cloud opacity, for scientific work. The data is based on various satellite images and weather models and thus offers a further point of comparison to the self-collected data and the data from the Solar Atlas Hamburg. In this thesis, data on cloud opacity is mainly used to contextualize the solar data collected in the evaluation chapter.

7 Evaluation

In this chapter, the measurement data collected as part of this thesis is systematically evaluated and compared with the reference data set of the Hamburg Solar Atlas. The focus is on answering research question Q1 and determining to what extent it is possible to evaluate the large-scale solar data set and, highlight problems with it.

Several scenarios were carried out to answer this question in which the solar modules presented in the implementation chapter were used to gather precision solar data. Different measurement points were explicitly chosen to evaluate the Solar Atlas under various influencing factors. The aim is to assess the data contained in the Solar Atlas and highlight existing deviations. Additionally, at the end of this chapter, the requirements set out in chapter 4 are evaluated to determine whether they have been met in this thesis.

7.1 Detailed Scenario Analyses

The individual test scenarios carried out as part of the evaluation are presented below. Each scenario is designed to directly answer a specific question regarding the evaluation of the Solar Atlas and or to fulfill a requirement set out in this thesis.

Each scenario follows a uniform structure: First, the test setup is described, followed by the presentation of the measurement data, a comparison with the Hamburg Solar Atlas, and external data is presented then, and at the end of each scenario, a discussion of the results takes place.

7.1.1 Test Period and Location

Due to this thesis's limited time period, all scenarios are based on collected data are restricted between 27.12.2024 and 01.04.2025. Furthermore, all measurements were carried out at the computer science campus of the University of Hamburg at Vogt-Kölln Straße 30.

An overview of the computer science campus can be seen in Figure 7.1. The following scenarios are limited to measurements on the roofs of buildings D, F, and H, whereby all roofs are flat and of different heights. Building F is the tallest on the entire campus, with five floors. Building D has two floors, and H is the smallest, with only one floor. Further local conditions are documented in the following scenarios if necessary.

Due to the limited measurement period, only the winter months are covered in the data in this thesis. In addition, the data is subject to a local bias, as all the measurements

Figure 7.1: Map of the computer science campus in Hamburg Stellingen with labeled buildings. [UHH25]

are carried out in relative geographical proximity. This means that a location bias cannot be ruled out even when measuring different roofs on the site.

7.1.2 Scenario 1: Consistency of the Solar Module Measurement Data

The primary goal of the first scenario is to show that the developed solar modules can produce comparable results, which is in part required by the requirement R3. Furthermore, this first scenario evaluates to what extent the measured solar data can be used to make statements about solar performance to decide which position is better suited for solar power generation.

Description of the Scenario

For the scenario, two prototypes of the solar module were set up inside directly at the window, on opposite sides of room F-531 on the fourth floor of building F. The windows were aligned to the east/south side and should gather sunlight in the morning and noon. The expected results were similar measurements of the two solar modules, which differed

only minimally due to the house's orientation. The entire measurement period was from 29.12.2024 to 16.01.2024.

To test the modules would measure significant difference, one of the solar modules was placed on the other side of the house in room F-509 for 3 days. One module was still on the east / south side, but the other was on the west / north side. As the sun in northern Germany is only visible in the early morning hours in winter and is usually already too low in the afternoon, it is to be expected that the first module on the east / south side generates significantly more electricity with the solar panel than the module on the other side of the house.

Figure 7.2: Positioning of the prototype solar modules for the first scenario, with respective pseudo-compasses to show the irradiation angles.

Figure 7.2 shows the positioning of the prototype solar modules. On the left in the slightly larger image, it can be seen that two modules are positioned along the window front for the first measurement to compare the similar solar data acquisition of different modules. The two images on the right show the three days when the prototype solar modules were placed on different sides of the house to show significant differences in solar data collection.

Each positioning image in graphic 7.2 has a pseudo compass in the top right-hand corner. This pseudo compass serve as an orientation for the direction from which the sunlight can hit the modules, which is marked with a red border around the compass. For the installation in this scenario, positioning the two modules on the same front (left in the graphic) is possible from the east/south direction and not from the other directions, as there are no windows. The same applies to the module, which can be seen in the center of the graphic. For the right image the irradiation is on the opposite side (west/north).

Presentation of the Measured Data

Figure 7.3 shows a section of 3 days of the measurement period in which the prototype solar modules were set up in the same room. As the sensor data is logged continuously, the diagram includes the 24 hours of each day. The days are described on the X-axis, with the first marker representing midnight at 00:00 and the second one 12:00. The Y-axis shows the power generation of the solar panel in milli watts. Modules 2 and 3 are

represented as red and blue curves.

It is easy to see that the two modules have very similar curves, except at around 10:00 on 08.01, when module 3 produced almost twice as much electricity as module 2 for a short period. The most electricity was generated in the selected section on 08.01 at 12:00 when both modules produced just under 160 mW of electricity.

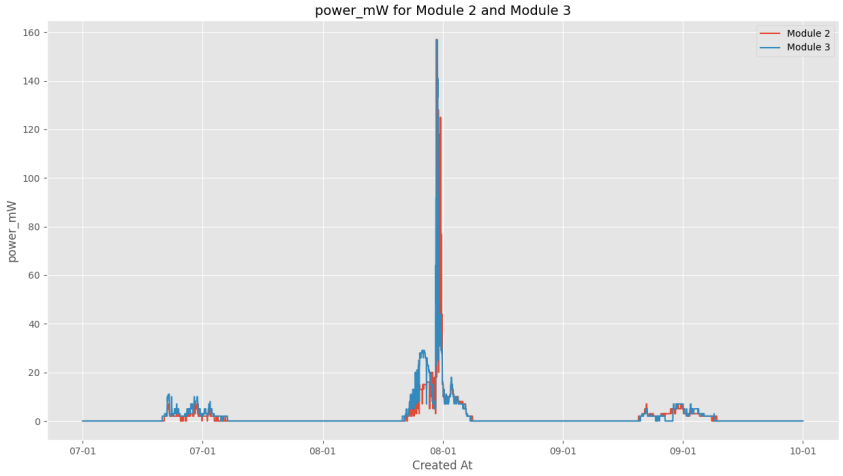

Figure 7.3: Power data evaluation from 07.01.25 to 10.01.25 of the two prototype solar modules, for the first presentation of the first scenario.

Figure 7.4 shows the 3-day period in which module 3 was placed on the opposite side of the house in another room. It is clear to see that module 3 only generated minimal power during this time. Module 2, on the other hand, produced significantly more electricity on all days during the measurement period, with almost 300mW. Its noticeable that on all 3 days, the electricity production of Module 2 drops abruptly around 12:00 and comes close to the values of Module 3. Furthermore, it can be seen in Figure 7.4 that Module 3 produces slightly more electricity than Module 2 in the afternoon. On 13.01 in the after noon, the electricity production of module 3 is noticeably higher than the production of Module 2.

The figure 7.5 and figure 7.6 show the respective temperature sensors installed in the modules. Although the temperature sensors are only secondary sensors of the modules, they help to provide even more context to the recorded sensor data. The temperature graphs are similar to the power generation graphs shown above. The only difference is the Y-axis, which shows the ambient temperature in Celsius at the measurement time.

Figure 7.5 shows the temperature curve for the measurement period shown in Figure 7.3. Here it can be seen more clearly that the two modules have very similar curves. Both modules recorded significantly higher temperatures on 08.01 and generally always measured a warmer ambient temperature at the 12:00 mark. In contrast, the temperature data for the second measurement in different rooms, which can be seen in Figure 7.6, show a significantly different temperature measurement of the modules. However, it can

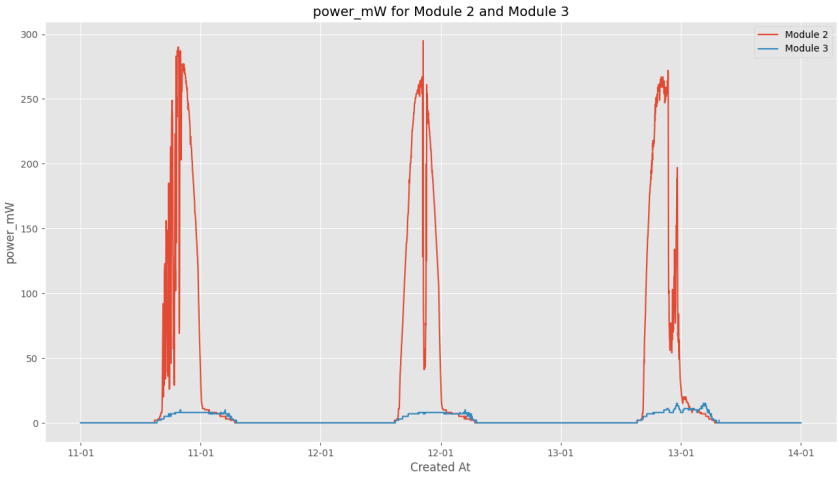

Figure 7.4: Power data evaluation from 11.01.25 to 14.01.25 of the two prototype solar modules, for the second presentation of scenario 1.

also be seen in this temperature graph that module 2 reaches its highest temperature at the 12:00 mark with a value of just over 23 degrees Celsius and then levels off. It can also be seen that Module 2 has more extreme values. Module 2 shows the daily low and high temperatures, whereas Module 3 shows a much more stable temperature curve.

Comparison with External Data

So that the measured data can be put into context, a diagram from the Deutscher Wetter Dienst (DWD) on the actual sun hours can be seen in graph 7.7. The X-axis displays the days of the measurement period, and the Y-axis shows the number of hours of sunshine recorded on each day.

For the first interval from 07.01 to 09.01, the DWD measured about 4.2 hours of sunshine only on 08.01. There was no or almost no solar radiation on 01.01 with 0.2 hours and 09.01 with 0 hours of sun. These results are consistent with the measured values of the modules shown in 7.3, which only recorded a significant peak on 07.01.

For the second interval, the period from 11.01 to 13.01 is to be considered. This period hast the most recorded sunshine hours seen in the data from the DWD. Here, the recorded values from module 2 of high solar radiation match the hours of sunshine seen in the date from the DWD. But the recorded data of no sunlight of module 3 for that period contradicts the total sun hours.

As this scenario is intended to compare the data collected from different solar modules and was primarily carried out indoors, the data from this scenario is not compared with the Solar Atlas.

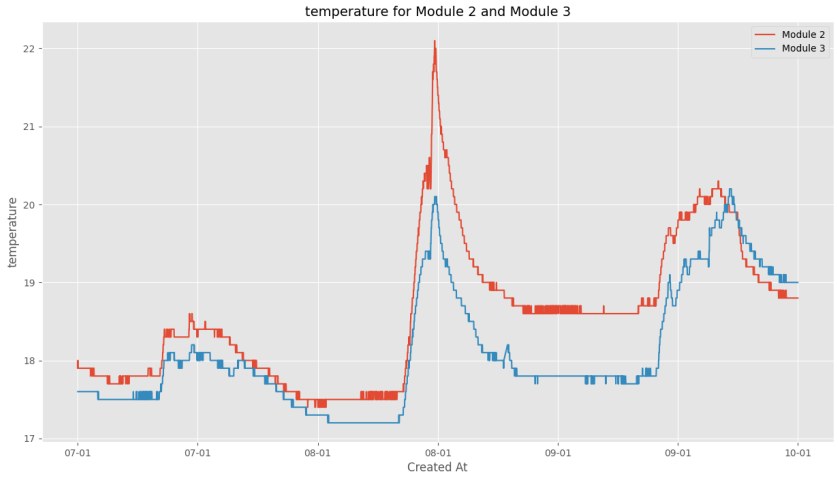

Figure 7.5: Temperature data evaluation from 07.01.25 to 10.01.25 of the two prototype solar modules, for the first presentation of scenario 1.

Discussion and Interpretation of the Results

The first scenario presented here answers research question Q2 by demonstrating whether the solar module developed in the implementation can collect meaningful precision solar data. To achieve this, two prototype solar modules were placed at different positions inside to compare the collected solar data with each other and with external data.

Considering external data such as the hours of sunshine from the Deutscher Wetter Dienst, the solar data that the modules recorded reflects the real conditions. Thus, they can capture and persist statements about the possible solar power generation at precision positions.

The precision aspect becomes clear when comparing the data in the opposite rooms in the same house. For example, module 2 could produce electricity, but module 3 could not because it was oriented the other way. This can also be seen when the solar power production of module 2 always drops at noon. Which can be explained by the sun's position facing south at 12:00, which means it can no longer directly reach the west-facing window.

Furthermore, the precision solar data acquisition can also be seen by the low power generation of module 3 seen in figure 7.4. Although the DWD recorded around 6 hours of sunshine on the measurement days, module 3 did not generate any significant solar energy. The low results can be explained by the winter months and the associated low sun. As the window faces west / north, the sun is already too low to shine directly on the module.

The solar module was still a prototype during the measurement, so it had to be placed inside. Therefore, the measurement results are not directly comparable with the Solar Atlas, as the dataset contains only roof data. This scenario could be improved when the

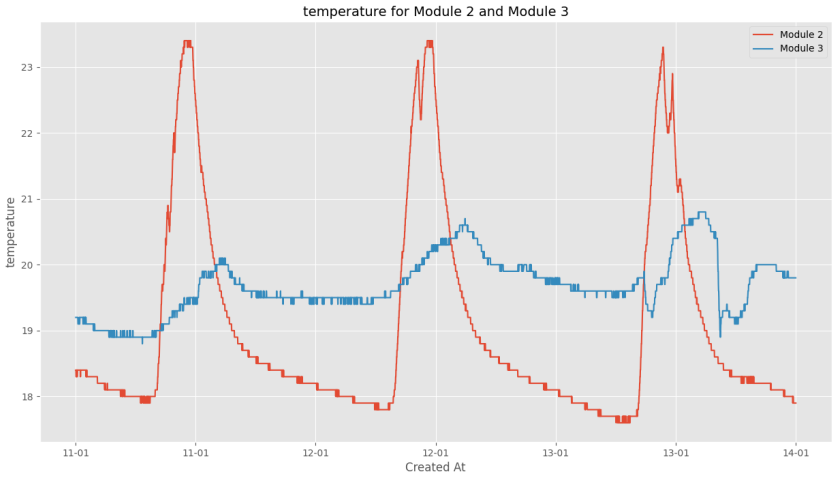

Figure 7.6: Temperature data evaluation from 11.01.25 to 14.01.25 of the two prototype solar modules, for the second presentation of scenario 1.

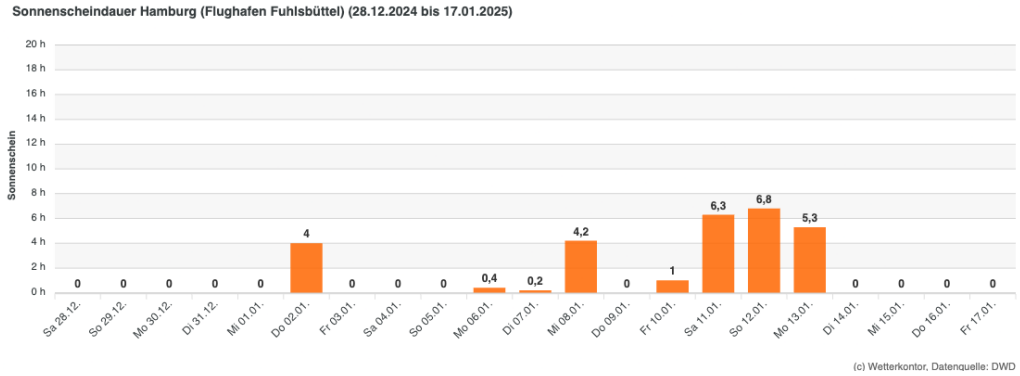

Figure 7.7: Recorded solar hours from the weather station of the Deutscher Wetter Dienst at Fuhlsbüttel Airport between 28.12.2025 and 17.01.2025. [wet25]

data could be used for direct comparison with the Solar Atlas and thus be able to conduct initial evaluations for the first research question Q1.

Furthermore, the time limit only covers a period of two weeks. Although this is enough time to establish a relationship between the measurement results and the hours of sunshine per day, it is not enough to determine trends based on the data alone. In addition, there is a local bias, which cannot be ruled out as the measurements were only carried out in two rooms in one building.

Finally, the data obtained is unsuitable for a general interpretation, as the measured solar energy values were recorded behind windows and are, therefore, not as high as when the solar panels are exposed to direct sunlight.

Nevertheless, Scenario 1 showed that the modules can record precision values for solar energy production even in limiting environments. Furthermore, the collected data from the solar modules can be compared, fulfilling this scenario's goal.

7.1.3 Scenario 2: Analysis of Local Irradiation Differences within a Roof

The second scenario aims to establish an initial reference to the heat map data of the Solar Atlas. This scenario will show that assumptions made with the help of the heat map can be confirmed with the precision data. Thus, the scenario is part of the answer to the initial research question Q1 to see to what extent the Solar Atlas can be evaluated with the help of collected solar precision data.

Establishing the initial relation between measured data and the heat map is necessary as the city provides no concrete information on the heat map's specific color values. Therefore, the first step is to show that red areas are more suitable than yellow or blue areas and that this assumption is correct.

Description of the Scenario

To implement this scenario, three prototype solar modules were set up on the roof of house F at the computer science campus from 29.01.25 to 13.02.25. For this purpose, the heat map shown in Figure 7.10 was used as a reference, and three different color areas were selected to determine values for those colors.

Furthermore, various local characteristics were examined that could result in discrepancies between the heat map and the actual measured precision solar data.

The exact positioning of the modules can be seen in Figure 7.8. The last four characters of the respective modules MAC addresses were used for identification, which also matched the following graphics of the data and their positioning in the respective scenario.

Figure 7.8: Positioning of the prototype solar modules for the second scenario, with respective pseudo-compasses to show the irradiation angles.

The first module, a6:44, is the first solar module to cover the blue color range of the heat map. The special feature of the positioning of the first module can be seen in graphic 7.8. In this graphic, the module is on the far left, which shows that the module was placed in a shaded corner of the roof next to many other components. The second module is module 53:89, placed in the heat map's yellow area. Again, a local peculiarity cannot be seen on the heat map alone. In the middle graphic 7.8, it can be seen that the module was

placed next to a distribution box, which, according to the heat map, should only have a moderate effect on power generation. The third module, 4b:oc, is placed in the red area of the heat map and has no special features except for a small heating pipe, which can be seen on the far right of the figure. In this scenario, the pseudo compasses of the respective positioning graphics again show the possible sunlight angles.

In the second scenario, prototypes of the solar modules were used to carry out the measurements because, due to time constraints, the measurements had to be carried out before the production-ready modules were available. However, since these were set up outside this time, the results are comparable with other results by the finished solar modules.

Presentation of the Measured Data

In the graphic 7.9, a section of the data between 31.01 and 02.02.25 is shown. The different modules are each marked with different curves and color. The X-axis shows the days, each with two markings for 00:00 and 12:00. The Y-axis shows the generated current in mW at the time of measurement.

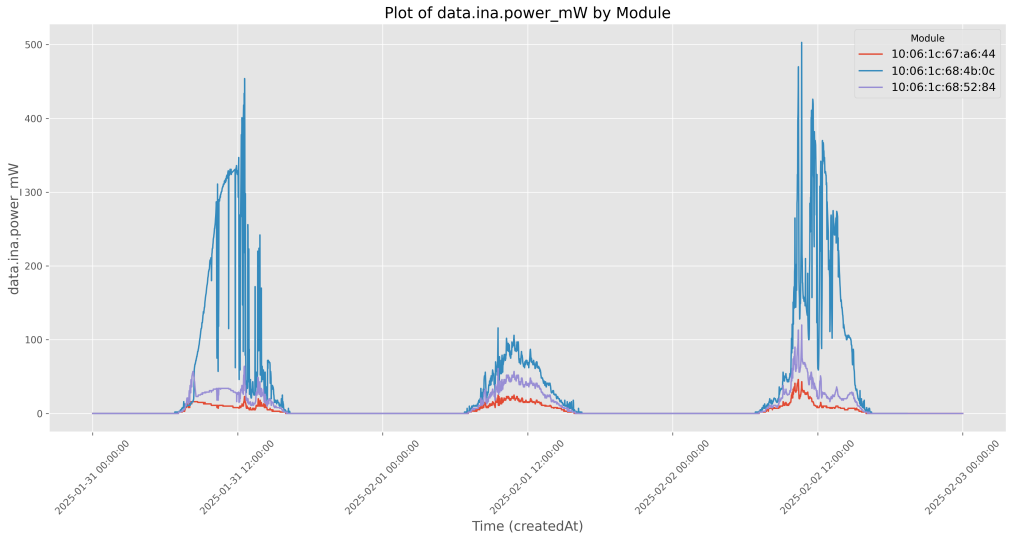

Figure 7.9: Power data evaluation selection between 31.01.25 to 03.02.25 of three solar modules of the second scenario.

Solar module 4b:oc generated significantly more power than the other two modules. With a peak value of over 500mW, the module exceeds all previously achieved power values. According to the data, module 52:84 is the second best module, with a power generation significantly below the 4b:oc module, but still, on average, twice as high as the power generation of module a6:44. Compared to the other two modules, module a6:44 generates the least power.

The ratio of the individual modules changing daily is notable in the data interval shown in Figure 7.9. While the 4b:oc module generates significantly more electricity than

the other modules on 31.01 and 02.02, is the power generation difference less significant on the 01.02. By contrast, the power generation ratio between the other two solar modules does not change over the three days.

Comparison with External Data

When the results are compared with the heat map colors, it is clear that the red areas are best suited for solar panels, whereas the yellow and blue areas are unsuitable for solar production.

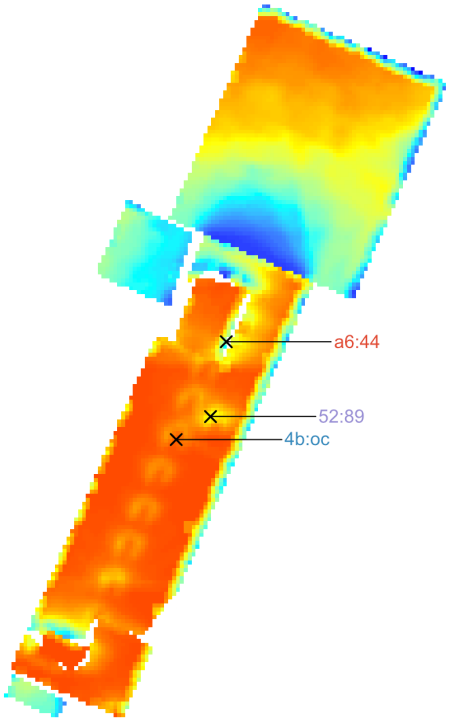

Figure 7.10: Heat map from the raw data of the Solar Atlas Hamburg with the position of the modules for the second scenario marked on it.

Comparing the data recorded in diagram 7.9 with the hours of sunshine from the DWD, as shown in graphic 7.11, it becomes clear that on the 01.02.25 was no sunshine. The sun did shine on the other two days, and therefore, the results for these days are usable for a comparison with the heat map of the Solar Atlas.

To better interpret the peaks in the measurement, the data from diagram 7.9 with the recorded cloud density from the Solcast API can be taken into consideration. What can be seen in the diagram 7.12 is the cloud density in percent on the Y-axis and the time of measurement on the X-axis. It should be noted that the Solcast API's data resolution is only hourly, whereas the resolution of the measurement data is every minute.

Nevertheless, a data comparison shows that the cloud density was also consistently high on 01.02, where the DWD registered no sunshine hours. On the other two days,

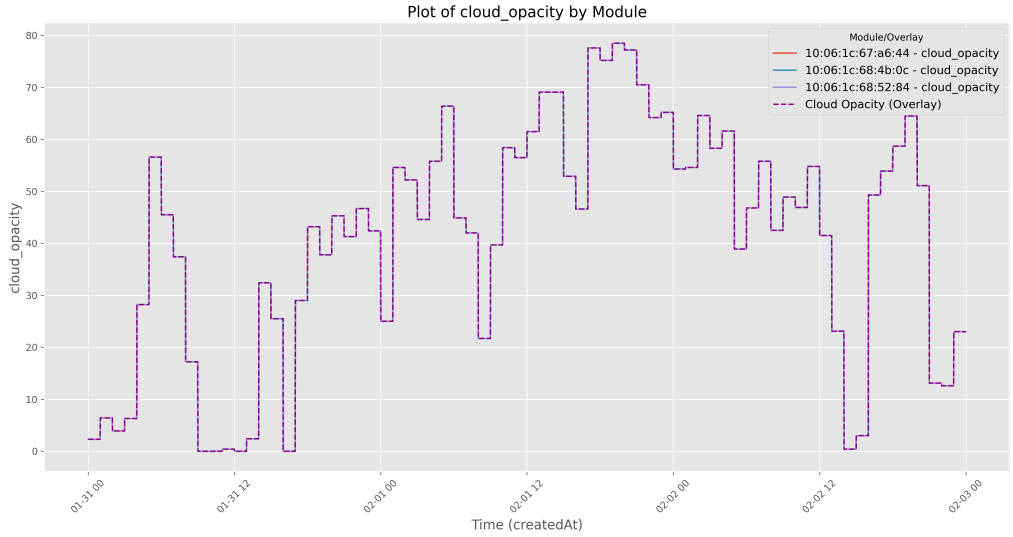

Figure 7.11: The recorded cloud density from the data of the Solcast API for the geo position of the computer science campus from 31.01.25 to 03.02.25 in one-hour measurement intervals.

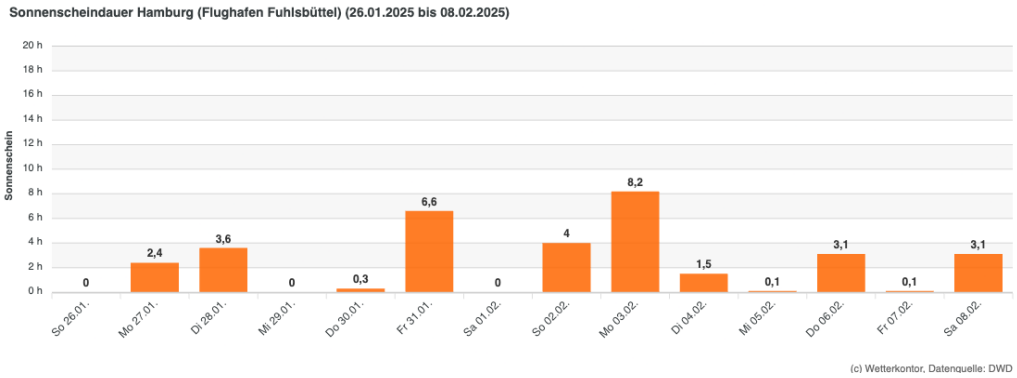

Figure 7.12: Recorded solar hours from the weather station of the Deutscher Wetter Dienst at Fuhlsbüttel Airport between 26.01.2025 and 08.02.2025. [wet25]

however, it was below 50%.

Discussion and Interpretation of the Results

The goal of this scenario was to show a relation between the heat map data of the Solar Atlas and the gathered data from the solar modules. The relation can then be used as a reference point for evaluating the Solar Atlas. A relation between the sensor data and the heatmap was successfully shown by demonstrating that the red areas of the heat map are better suited for solar power production than the yellow areas, which in turn are better suited than the blue areas.

The performance differences of the solar modules under good and bad conditions are noticeable. As can be seen, the difference in solar power generation under poor conditions, such as on 01.02, is present but significantly lower than when the sun is shining,

as seen on the other two days. It is interesting that the performance difference between modules a6:44 and 52:84 remains the same even on days with sufficient hours of sunshine and that both modules behave similarly.

The consistent difference, even on days with sunshine hours, directly contradicts the heat map data of the Solar Atlas, according to which the a6:44 module should be significantly less suitable for solar energy than the 52:89 module. However, the data shows that the module 52:89 is better suited, regardless of whether the sun was shining. Furthermore, the data from the yellow area suggests that the yellow areas are significantly less suitable for solar power installations than one might initially suspect. If one assumes that the color gradient reflects a linear performance, yellow regions should not be perfect, but they are still okay. However, the recorded measurement data shows that even the area measured here is unsuitable for solar production, even on sunny days, with a maximum of 100mW.

Another aspect is the positioning of the modules, which has already been mentioned in the scenario description. The Solar Atlas does not contain any information about obstacles that make setting up a solar power plant impossible. Thus, realistically, solar power plants cannot be set up at two of the three selected positions, which can be seen in the middle and left images of graphic 7.8. However, this information cannot be obtained from the Solar Atlas data.

It cannot be ruled out that the measurements carried out are influenced by a local bias since only one sensor was set up per color zone. In the larger context, however, the entire roof of house F could also be a local anomaly. To rule this out, additional measurements must be carried out on several roofs to confirm these assumptions.

For the evaluation of Solar Atlas, it is therefore interesting to know whether these data are only a local bias or whether there is a more systematic difference compared to real measurement data.

7.1.4 Scenario 3: Validation of Measurement Consistency under Identical Conditions

The third scenario aims to evaluate the extent to which the same measurement values can be achieved in the red area of the heat map. Thus, this scenario contributes to research question Q1 which is to evaluate the Solar Atlas and analyse whether the red areas show significant differences or are equally suitable.

Description of the Scenario

To check the different red values of the heat map, four solar modules were placed on the roof of house F of the computer science campus between the 27.02.25 and 05.03.25. Only red areas were selected because they guarantee a good position according to the Solar Atlas. The exact positions were marked in the heat map 7.14.

When setting up the sensors, care was taken to ensure they were not surrounded by objects or other obstacles that could cast shadows. Therefore, all sensors have almost all-round coverage of solar radiation.

Presentation of the Measured Data

The diagram 7.13 shows a section of two days of the measurement period. On the left side of the diagram on the 02.03, the red, blue, and gray modules have achieved the same measurement results. Except for the afternoon hours, around about 16:00, when the blue module generates more electricity than the other modules. The purple module has a similar curve throughout the day. But only that module generates significantly less electricity than the other modules. In addition, with a peak of 200mW, not all modules generated much electricity.

The next day, shown on the right in diagram 7.13, indicate significantly larger measured values. The curve of the individual modules is no longer congruent and sometimes varies significantly between isolated measurements. Nevertheless, it can be seen that all four modules follow the same trend on this day. Only the purple module generates substantially less power than the rest. Furthermore, the red module generated less power than the other modules at the beginning of the day and stopped generating power altogether at around 2:00 p.m. In general, there is more variance in the results on the second day than on the first day of the interval shown. The blue, red, and gray modules reach the power generation peak of about 600mW, which happens at noon.

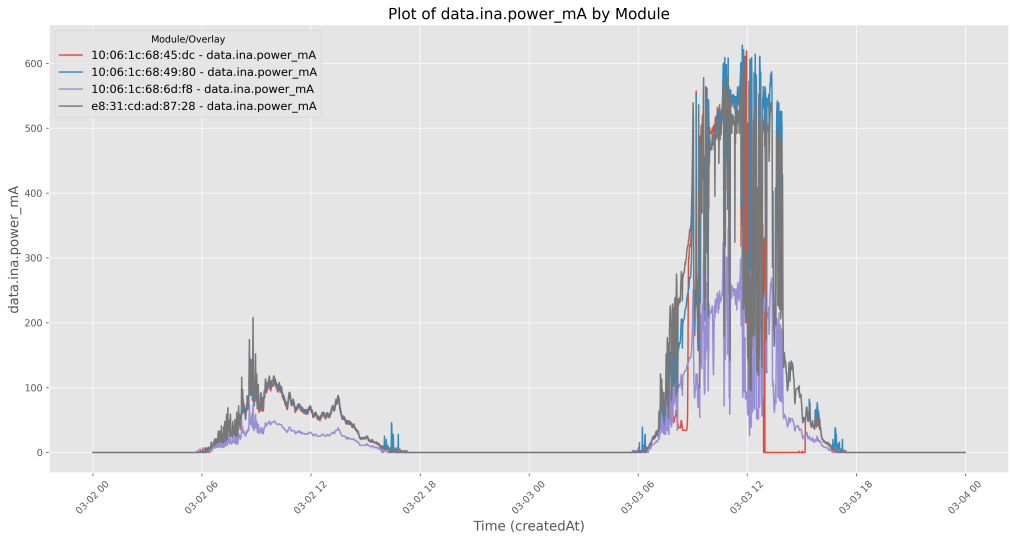

Figure 7.13: Power data evaluation selection between 02.03.25 to 04.03.25 of four solar modules of the third scenario.

Comparison with External Data

Comparing the data from the interval shown in figure 7.13 with the positioning data on the heat map of the Solar Atlas, shows that the purple module 6d:f8 was positioned on an equally red spot as the other modules.

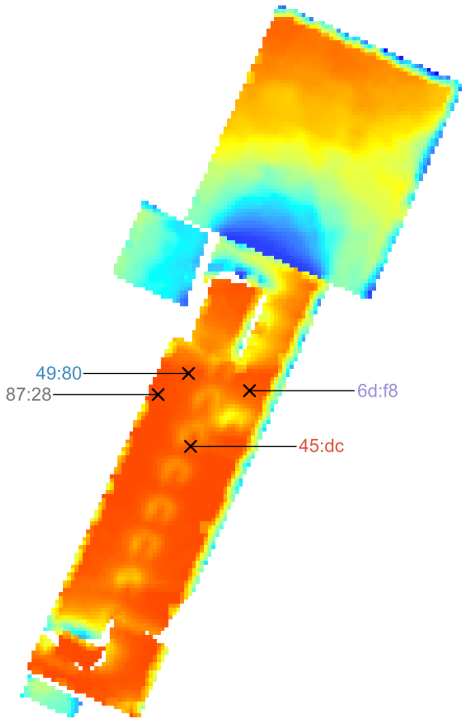

Figure 7.14: Heat map from the raw data of the Solar Atlas Hamburg with the position of the modules for the third scenario marked on it.

The graphic 7.15 shows the cloud density for the two measurement days of the displayed interval, with the X-axis representing the two days in 6-hour sections and the Y-axis representing the cloud density in percentage. A direct comparison of the measurement data shows that on 02.03, the density of the clouds was extremely high compared to the other days.

The high cloud density is also confirmed by the data from the DWD in Figure 7.16, which did not record any sunshine hours for that day. However, it can be seen that on 02.03, between 07:00 and 08:00, the cloud density briefly flattened out and was only just under 35%. This can also be seen in the power output of the data in graphic 7.13 at the same time. What is important here is that all modules, even the one that appears to be in a suboptimal location, used the spike to generate electricity.

The second day of the measurement interval shows lower values for cloud density in the morning and midday hours, corresponding to the data recorded by the DWD with 5.1 hours of sunshine on that day and the maximum values measured by the modules.

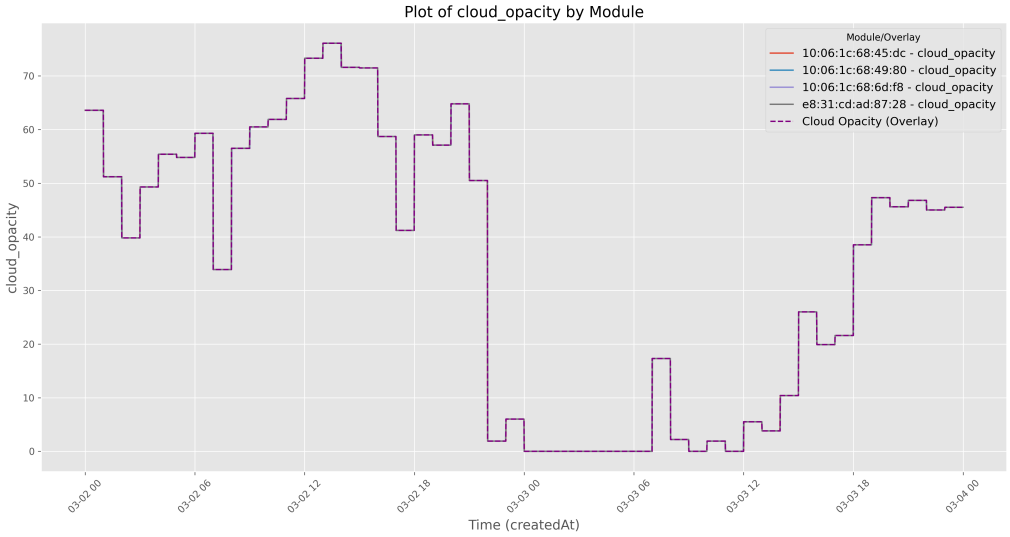

Figure 7.15: The recorded cloud density from the data of the Solcast API for the geo position of the ncomputer science campus from 02.03.25 to 04.03.25 in one-hour measurement intervals.

Discussion and Interpretation of the Results

This scenario aimed to evaluate how well the Solar Atlas represents the extreme good positions and whether all the red areas shown on the heat map have the same measured values. The data collected showed that the solar modules set up in the red areas of the heat map delivered almost identical results, especially on a non-sunny day. However, there was variance in the data when the solar modules were directly in the sun.

There may be several reasons why the purple module performed worse throughout. The most likely reason is that a local anomaly on the roof cast an unexpected shadow on the module. It is also possible that the module was at a slight angle when installed since even flat roofs are not always complete flat in all places. Furthermore, a hardware error cannot be ruled out at that point.

However, the Solar Atlas may show incorrect values at the position of the purple module. To determine this definitively, it is best to repeat this scenario on a different roof under similar conditions to evaluate where the problem with the deviating data came from.

The deviation shown by the red module on day two of the measurement interval is likely attributed to a hardware error or a local problem on the module. For example, a obstruction on the solar panel of the module could limit its performance, which would explain the slight deviation at the beginning of the second day. However, the module's failure to generate electricity in the afternoon of the second day is probably due to a sensor error, especially when the blue and gray modules, that show an identical measured value at this point, are considered.

To answer the research question Q1, it can be stated that the heat map is similar in the

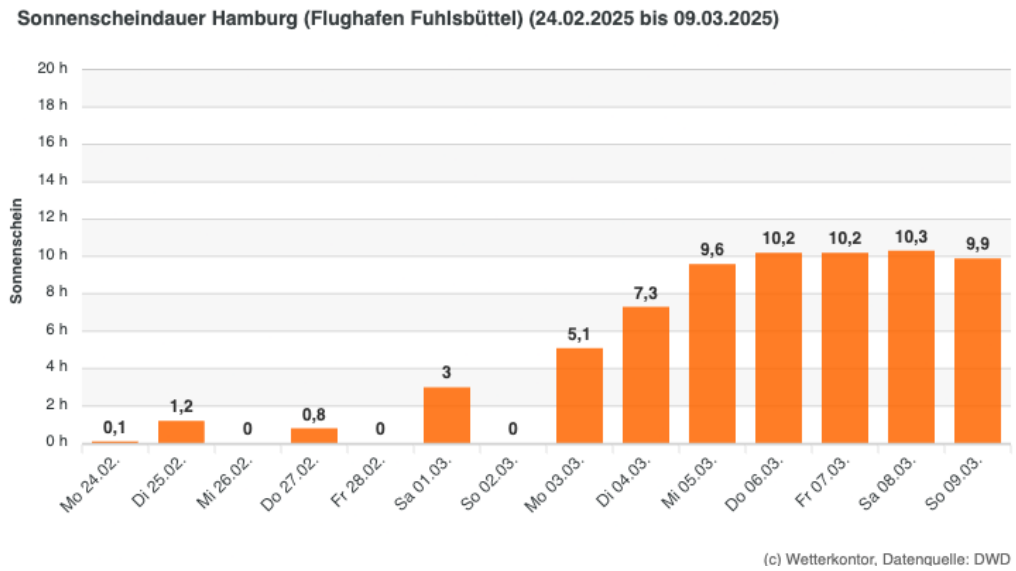

Figure 7.16: Recorded solar hours from the weather station of the Deutscher Wetter Dienst at Fuhlsbüttel Airport between 24.02.2025 and 09.03.2025. [wet25]

red areas, and it can be assumed that a red value on a roof is identical to all other red areas. Nevertheless, it must be checked whether this is only local equality, i.e., the colors per roof reflect the same values, or whether similar colorings of the heat map on different roofs express the same value.

7.1.5 Scenario 4: Comparison of measurement accuracy for equally rated heat map areas on different buildings

To exclude the possibility that the red area values from scenario 3 behave the same only because of a local bias, scenario four compares equal color ranges of the heat map on different roofs. This way, it can be evaluated whether the same values for different roofs mean the same or whether there are distinctions.

The scenario is carried out to answer research question Q1 to evaluate the Solar Atlas. This scenario allows a general statement to be made about the Solar Atlas data and excludes errors due to a local bias of a single roof.

Description of the Scenario

To carry out the scenario, four solar modules were set up on three different roofs of the computer science campus between 06.03.25 and 17.03.25. Two modules were positioned as a reference on the roof of Building F in already established red positions. The other two modules were set up on the roof of house C of the computer science campus to achieve the most distance between the roofs. The 45:dc module was placed on the main roof of the building C in a comparable red area. The fourth module 87:28 was placed on a small roof on the access hut of building C, in a red area of the Solar Atlas. The exact positions

are shown on the heat map graphic 7.18.

Presentation of the Measured Data

In diagram 7.17, a section of the measurement period from 08.03.25 to 10.03.25 can be seen. The days and times are shown on the X-axis, the power production on the Y-axis, and a graph in a different color for each module. It can be observed that all modules on all three days achieved peak values for power generation of around 500mW. Furthermore, it can be seen that all modules have a very similar curve.

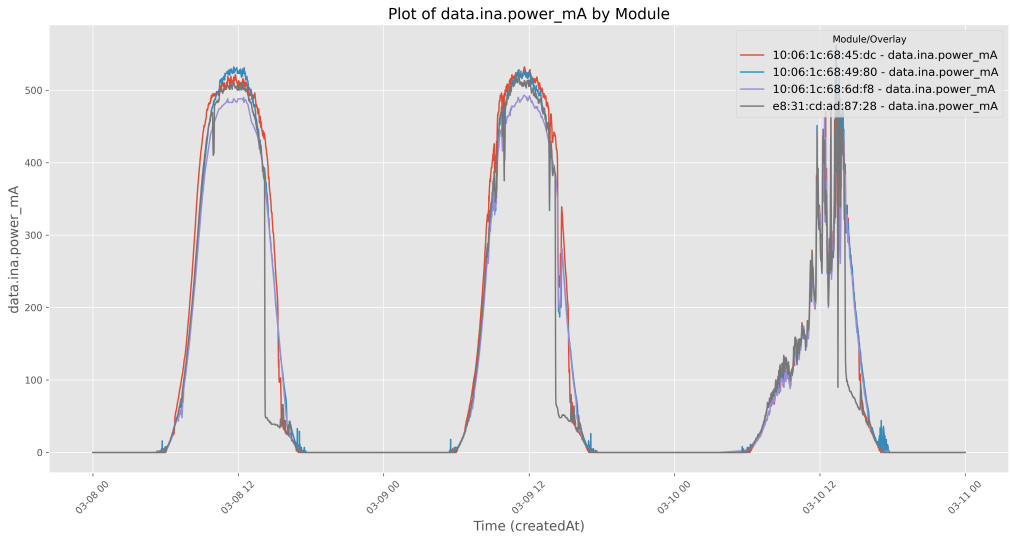

Figure 7.17: Power data evaluation selection between 08.03.25 to 11.03.25 of four solar modules for the fourth scenario.

When directly compared, the purple module 6d:f8 performs worse than the other modules. This can be seen from the fact that the purple module does not reach the 500mW limit for the day. However, the purple module's power production appears identical to that of the other modules at different times of the day.

The first two days have a very even trend, whereas the third day, shown on the far right of the diagram, has a rather abruptly rise and fall. In general, there is significantly more variance in the results on the third day.

When looking at the gray module 87:28, it is noticeable that the power generation drops faster on all three days than for the other modules. However, this drop is only lasting for one to two hours, and the module drops again in parallel with the other modules.

Comparison with External Data

Compared to the heat map data in figure 7.18 from the Solar Atlas, it can be seen that the same colors on different roofs match. Nevertheless, some local factors at the position would make some positions better suited. This can be seen from the different maximum

readings for the respective modules and from the deviation of, the gray module at the end of the day. However, these impacts of local factors are not visible in the heat map.

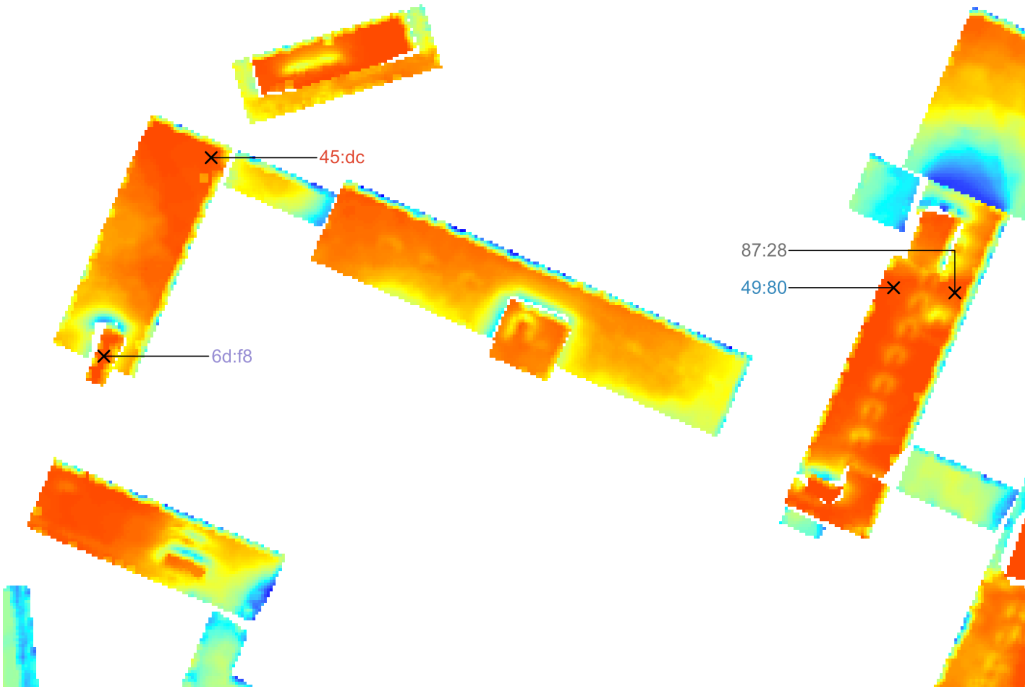

Figure 7.18: Heat map from the raw data of the Solar Atlas Hamburg with the position of the modules for the fourth scenario marked on it.

In the graphic 7.19, the cloud density from the Solcast API for the time interval can be seen. Here, it is initially noticeable that the third day had a lower overall cloud density, which would contradict the recorded data, which showed that the third day performed significantly worse than the days before. However, it is noticeable that the cloud density drop to zero at around 12:00. The figure also shows no cloud density at 08:00 on the second day, and the modules could directly capture the entire sun throughout the day.

When looking at the sunshine hours data from the DWD in figure 7.20, one can see that on the first two days of the measurement interval, around 10 sunshine hours were recorded, which corresponds to the even and high value of the recorded data. However, the third day had only 3.3 sunshine hours, which is cohesive with the recoded cloud density data.

Discussion and Interpretation of the Results

This scenario evaluated how the same heat map areas on different roofs behave. The data collected from the modules showed that under ideal conditions, the solar modules trends and real measurement values were similar.

It was noticeable that despite the modules being installed in the same areas, measur-

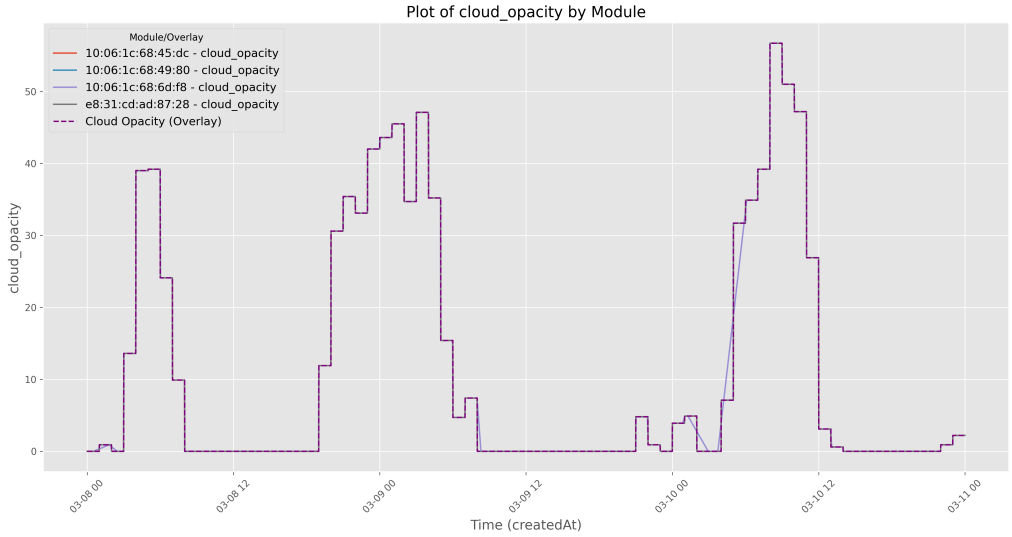

Figure 7.19: The recorded cloud density from the data of the Solcast API for the geo position of the ncomputer science campus from 08.03.25 to 11.03.25 in one-hour measurement intervals.

able differences between them were recognizable. This was most evident when the conditions were not ideal, as on day 3 of the measurement interval shown in Figure 7.17. This variance suggests that the Solar Atlas will become less accurate when conditions are not ideal.

In addition, local factors are still important in determining the perfect position. Even though the modules produced similar results, it is clear that the gray module 87:28 performs slightly worse than the other modules, which cannot be seen from the heat map data alone. Since it could be shown that non-ideal conditions can lead to greater variance at seemingly identical positions in the Solar Atlas data, it would be interesting to know how the data from the Solar Atlas behave at non-ideal positions. This should be checked to validate that different suboptimal areas in the data are identical.

7.1.6 Scenario 5: Checking the validity of the heat map for suboptimal solar locations on different roofs

The fifth scenario aims to evaluate how the data from the Solar Atlas behaves in suboptimal locations. It should be evaluated whether the statements of the Solar Atlas change in areas that are not good, i.e., red, or bad, i.e., blue. In addition, various factors can make an area only suboptimal for solar panels, and therefore, the different positions of the solar panels in these areas should be evaluated to determine how they affect the data. Furthermore, the other scenarios have shown that the Solar Atlas starts to lose accuracy in less optimal situations, so it is interesting to see to what extent the actual solar data differs from the seemingly identical positions. Thus, scenario five deals with research question Q1 and evaluates the Hamburg Solar Atlas in suboptimal situations.

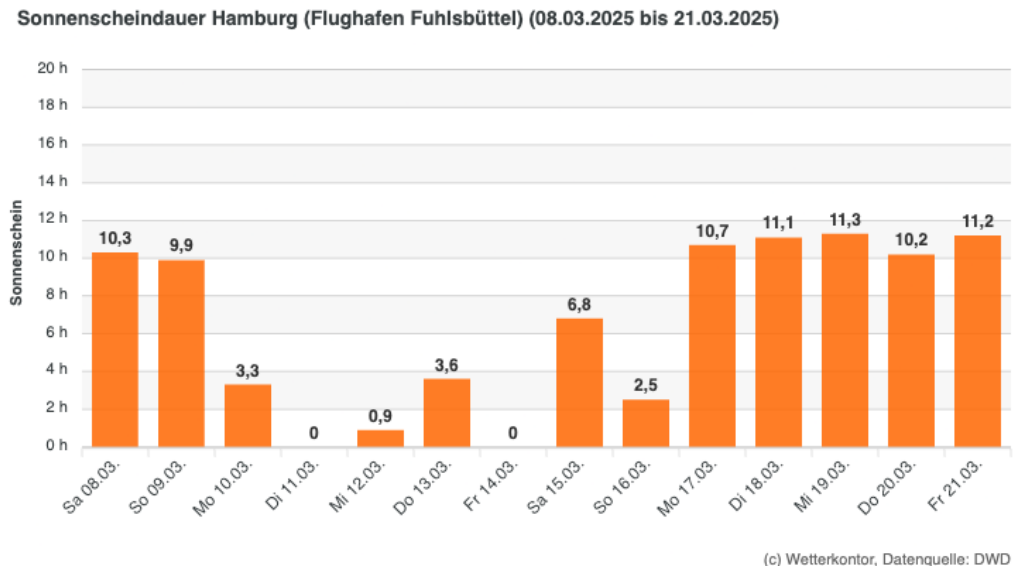

Figure 7.20: Recorded solar hours from the weather station of the Deutscher Wetter Dienst at Fuhlsbüttel Airport between 08.03.2025 and 21.03.2025. [wet25]

Description of the Scenario

To find less optimal positions, areas that are yellow or almost green on the heat map of the Solar Atlas were selected for the scenario. Four solar panels were installed on two roofs suboptimal areas of the computer science campus from 18.03.2025 to 27.03.2025. One of the modules was mounted on a yellow area of the roof of house F, which has already been used in other scenarios. This area is particularly interesting because solar radiation is limited due to local obstacle at this position. The three other modules were installed in suboptimal areas of house H. This single-story house stands between two buildings, F and G, and should not be optimally suited for solar panels, making it perfect for the scenario to be examined here. The exact position of each module can be seen in figure 7.23.

The special feature of house H is that different shadows are cast on the house depending on the time of day. However, since most sunlight occurs in the morning and at noon, one side of the roof should generate significantly more electricity than the other and thus be better suited for a solar power installation. But at that location the corresponding heat map indicates that the roof looks equally suitable for a solar panel, which this szenario aims to validate.

Presentation of the Measured Data

In the graphic 7.21, the entire measurement period of all installed modules is displayed. The results are smoothed by a moving average with a window size 60 to make the graphs more readable. That means the the following 60 data points (i.e., one hour of measurement) of each measurement are summed up and averaged before it was displayed. This

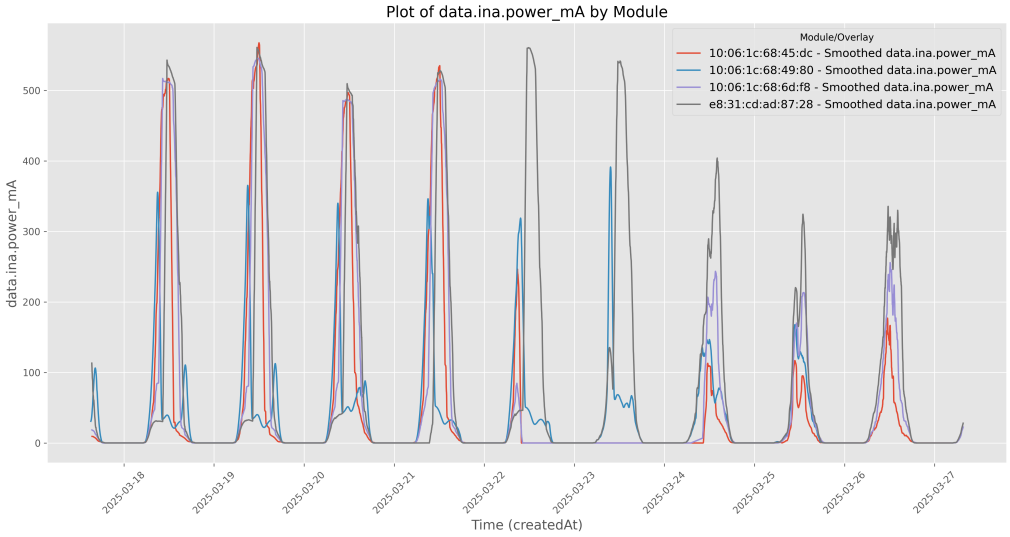

Figure 7.21: Power data evaluation of the complete measurement period between 18.03.25 to 27.03.25 of four solar modules of the fifth scenario, smoothed with a moving average of 60 measurement points.

was done for each measuring point.

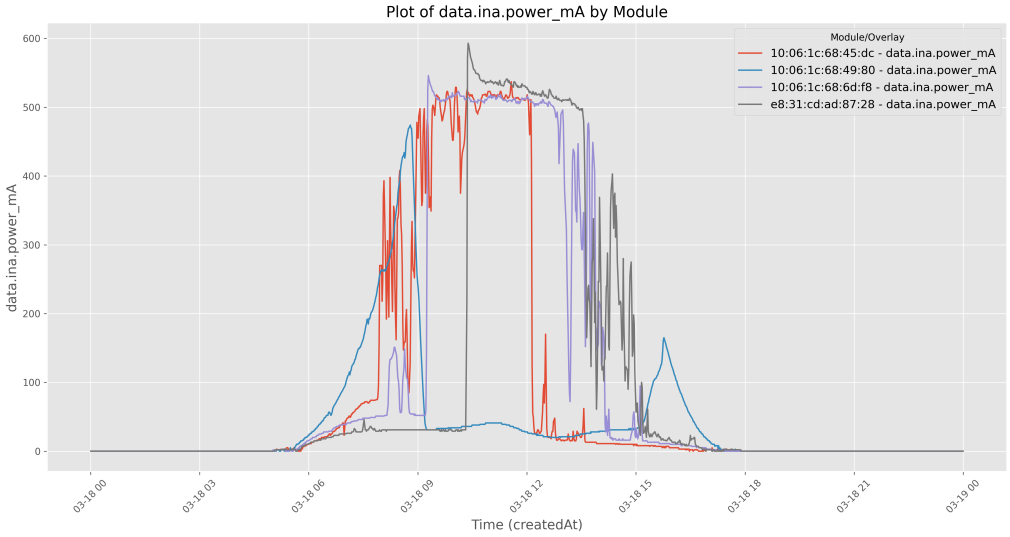

Figure 7.22: Detailed power data evaluation of the 18.03.2015 of all four modules for the fifth scenario.

As seen in graphic 7.21 that all of the modules have different results over the measurement period. The blue module performed worst on average, whereas the gray, red, and purple modules appeared to have better results. However, detailed information is important for differentiation between the modules which has been lost by smoothing the results. Furthermore, the red and purple modules did not record any data between March 22 and March 24.

In figure 7.22, the power data of March 18 can be seen in detail without smoothing.

Here, the apparent differences between the modules can be observed. It is easy to see that in the morning hours, the red and blue modules start to generate electricity, with the blue module stopping again shortly before 9:00. At around 9:00, the purple module suddenly starts to generate electricity and remains at the same level as the red module. This is followed shortly after 10:00 by the gray module, which generates even more power than the other modules and reaches a peak value of almost 600mW. Furthermore, the modules start to generate less power again at different times and in different stages throughout the day. It can also be observed that the blue module starts to generate electricity again shortly after 3:00 p.m., whereas the other modules have already stopped.

Color	**Module**	**Total Energy (mWh)**
Red	10:06:1c:68:45:dc	2000.33 mWh
Blue	10:06:1c:68:49:80	947.59 mWh
Purple	10:06:1c:68:6d:f8	2470.39 mWh
Gray	e8:31:cd:ad:87:28	2176.26 mWh

Table 7.1: Total energy measured by the solar module on the 18.03.25

In the figure 7.1, a tabular list of the solar module's generated electricity values from the measurement day shown in Figure 7.22 can be seen. The blue module generated the least electricity at under 1000mWh. The other modules have all generated more than 2000mWh of electricity, with a difference of 10% between the red and gray modules. The purple module has generated 25% more electricity than the red module, which is a significantly higher result.

Comparison with External Data

The position of the modules on the heat map shows that the blue module was placed in a rather yellow area, the gray and purple modules are in a yellow-green area, and the red module is in a green area. However, compared with the data from the measurements in Figure 7.22, it can be deduced that the blue module performed the worst of all modules, contrary to what the Solar Atlas had predicted.

This becomes even clearer when the actual values of the total electricity production of the individual modules from table 7.1 are considered. Here, it is clear that the blue module has performed the worst, which contradicts the heat map's statement. In addition, although the heat map colors for modules 87:28 (gray) and 6d:f8 (purple) hardly differ, there is a measurable difference in the performance.

The data from the DWD 7.25 show that the measurement day of 03/18 was an average sunny day with over 10 hours of sunshine, which should not have significantly influenced the measurements. This can be further confirmed with the cloud data from the Solcast API, seen in figure 7.24, since there was only a minimal cloud density in the early morning hours and otherwise the sky was cloud-free. Therefore, the measurements on 18.03 only deviate due to the modules' chosen positioning and are ideal for comparing

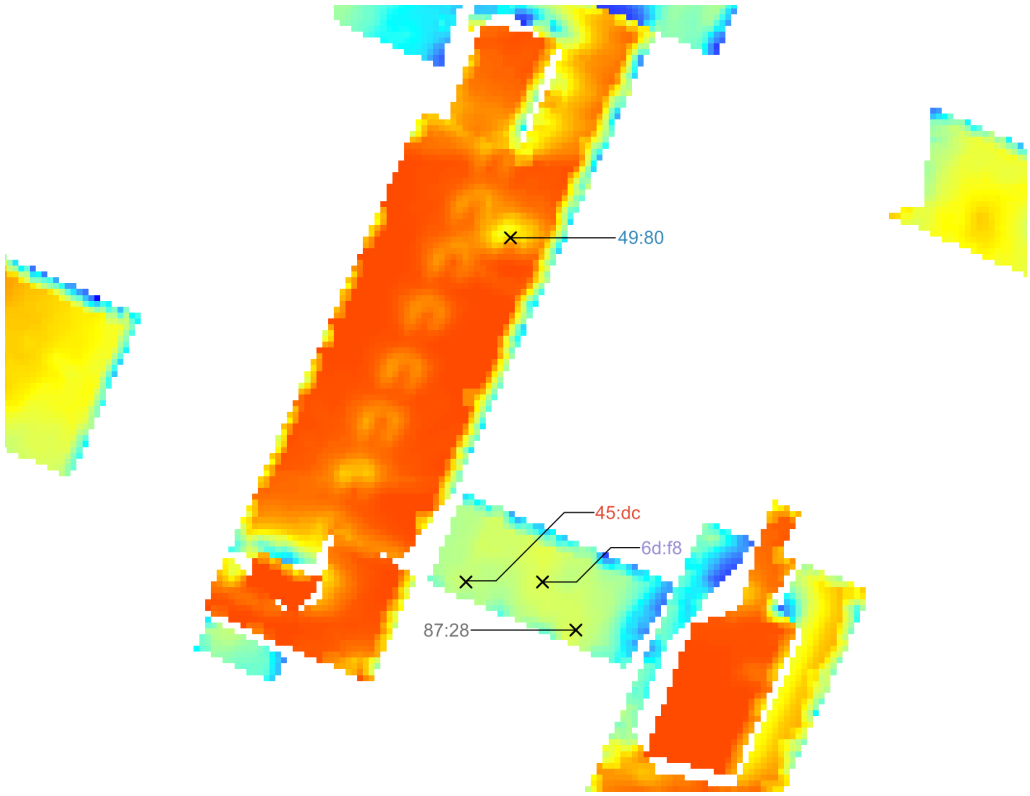

Figure 7.23: Heat map from the raw data of the Solar Atlas Hamburg with the position of the modules for the fifth scenario marked on it.

with the predicted data from the Solar Atlas.

Discussion and Interpretation of the Results

Scenario 5 was designed to evaluate whether the suboptimal positions, i.e., the yellow areas of the Solar Atlas, lead to inaccurate measurement results, as suspected. By measuring several optimal areas it could be shown that the Solar Atlas is sometimes inaccurate and cannot provide a clear statement about the best suboptimal position for a solar panel.

The blue module (49:80) shows the most significant contradiction. According to the heat map, this module was placed in the best of the four selected positions. However, the blue module performed the worst even under ideal measurement conditions. The red module on the roof of building H was expected to produce the least electricity since it was placed in an already rather green area of the heat map. However, even the red module generated more than twice as much electricity as the blue module, which is an apparent contradiction to the predictions of the Solar Atlas.

Considering the previous scenarios, this is probably because local features at the measuring points, such as the junction box on the roof of the house F next to the blue module, were not considered when creating the Solar Atlas. Since the data set was created over a large area, it lacks the resolution of the individual roofs to decide which position of a roof

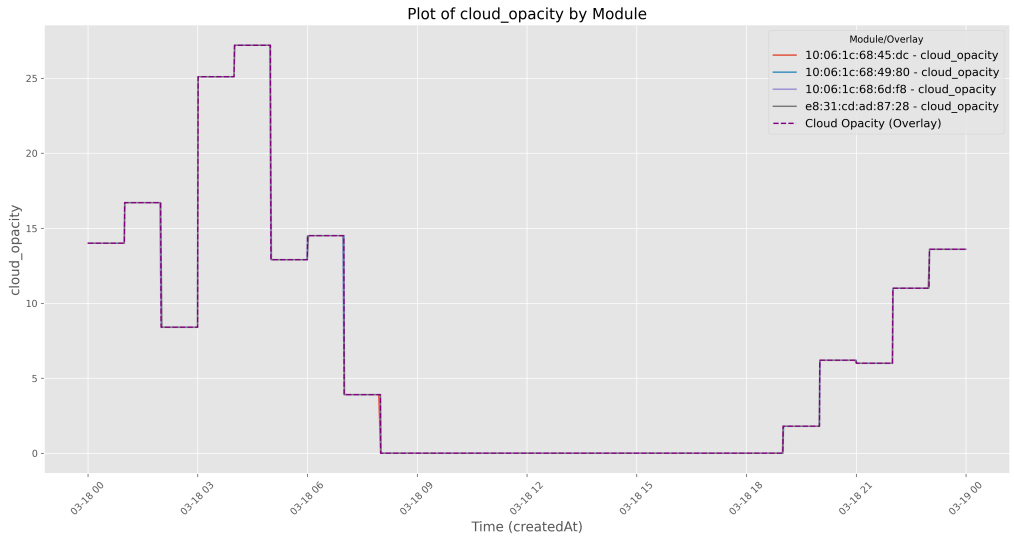

Figure 7.24: The recorded cloud density from the data of the Solcast API for the geo position of the ncomputer science campus from the 18.03.25 in one-hour measurement intervals.

is better in suboptimal conditions. This can also be seen from the fact that even modules on the same roof, such as the purple module and the gray one, have a power generation difference of about 13%, although this cannot be seen from the color of the position on the heat map.

The heat map as a medium to display the data is too inaccurate to clarify such differences. However, a production difference of 13% is not irrelevant when deciding whether a solar power plant on the roof could be worthwhile. Therefore, the evaluation of the Solar Atlas raises the question of whether the data set contains enough accurate data to make valid decisions about a possible purchase of a solar power installation.

7.2 Requirement Evaluation

In Chapter 4, requirements were established to serve as a basis for answering research questions Q1 and Q2. In order to provide answers to the research question, some requirements were addressed in detail in both the implementation and the scenario-based evaluation. However, some of the requirements are aimed at the overall system and have not yet been addressed. In this section, each defined requirement is considered individually and evaluated to determine the extent to which it has been fulfilled in the thesis.

Table 7.2 provides an overview of the requirements. It shows which requirements have been fulfilled, partially fulfilled, or not fulfilled. A more detailed evaluation of the fulfillment of each requirement is provided below.

The first requirement R1 specifies that a reference data set with solar data must be available for comparison with the collected precision data. As described in the implementation section 6, the Hamburg Solar Atlas was selected as the reference data set for

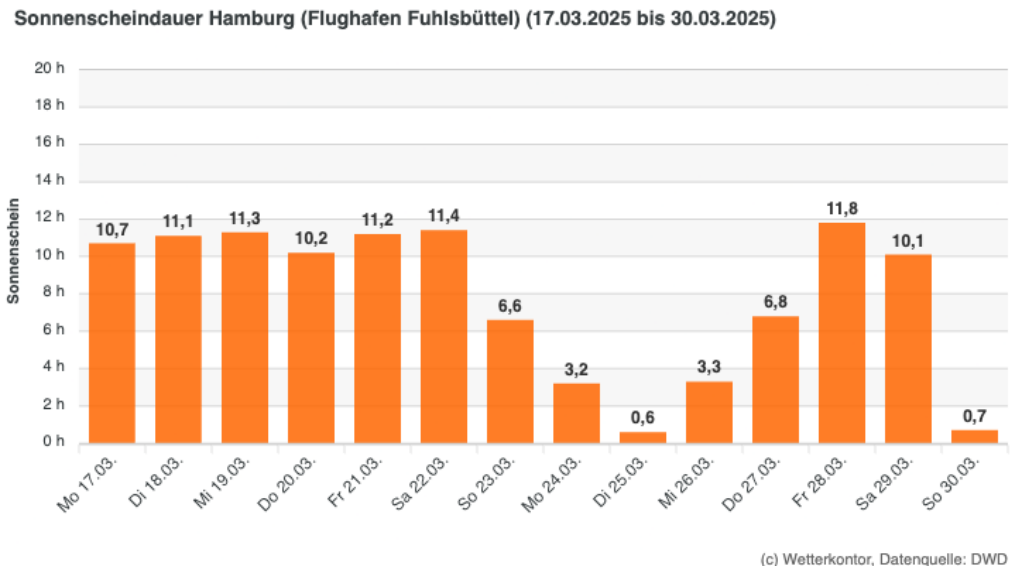

Figure 7.25: Recorded solar hours from the weather station of the Deutscher Wetter Dienst at Fuhlsbüttel Airport between 17.03.2025 and 30.03.2025. [wet25]

this thesis. The evaluation was successfully carried out using the raw heat map data in several scenarios. Although specific values for comparing specific points or areas were unavailable in the data set, the evaluation was successful, and insights were gained from comparing self-measured data with the Solar Atlas. Therefore, requirement R1 is considered to be fulfilled.

The second requirement R2, states that solar precision data should be able to be determined at specific positions. The scenarios showed that the solar module developed in the implementation phase could be used to gather solar date for specific precision points. Thus, requirement R2 has also been fulfilled.

Scenarios 2–5 were carried out to evaluate the Hamburg Solar Atlas directly. This means the third requirement, R3, which requires that the measured data is comparable with reference data, has been fulfilled. In addition, the sub-requirement from R3, which requires that the data be comparable between solar modules, was demonstrated in scenario one.

Requirement R4 requires that a measurement period to be selected that is long enough to collect sufficient data for the evaluation. For the respective scenarios, a measurement period of two weeks was selected to cover a period that is as large as possible within the limited processing time of this thesis. Ideally, the solar data would habe been collected for an entire year, and for each scenario to cover the different seasons and minimize anomalies. However, since an evaluation could be carried out even within a limited time period, requirement R4 is considered to be fulfilled.

Requirement R5 requires that the measured units to be comparable to those used in the reference data set. Since the Solar Atlas raw data set was only available as a heat map without specific values, a realistic setup was chosen to reflect the Solar Atlas data as well

Requirement	Fulfilled
R1	✓
R2	✓
R3	✓
R4	✓
R5	(✓)
R6	(✓)
R7	✓
R8	(✓)
R9	✓
R10	✓
R11	✓
R12	✓
R13	✓
R14	✓
R15	(✓)

Table 7.2: Overview of the requirement evaluation. The left column shows the reference to the requirement and the right column if the requirement is fulfilled. ✓= fulfilled, (✓) = partialy fulfilled, x = not fulfilled.

as possible. Since a sub-requirement was that meaningful statements should be able to be made, which could be done, this requirement counts as partially fulfilled.

Requirement R6 requires that different measurement points be used to avoid local bias. Different measurement points on different roofs were selected in the scenarios to meet this requirement. However, it cannot be ruled out that bias exists on the computer science campus, as only roofs one area were used for evaluation. For this reason, requirement R6 is only considered partially fulfilled.

Requirement R7 requires that no faulty data is to be used for the evaluation. Since most scenarios used only subsections of the respective measurement periods as evaluation bases, faulty data in those periods could be ignored when selecting those subsections. This requirement is therefore considered to be fulfilled.

Requirement R8 requires determining the extent to which the measured data differs from the data in the Solar Atlas. Furthermore, it is required to determine whether the differences are only local or only occur at certain times. Differences between measured and existing data were found, particularly in scenario 5. However, it was impossible to determine in more detail whether these differences only occur under certain circumstances, such as location and time, within the available time frame of this thesis. Therefore, this requirement is only partially fulfilled.

External factors should also be considered in the evaluation for requirement R9. For scenarios 2–5, data from the DWD on sun hours and values for cloud density from the Solcast API were used. Therefore, this requirement is considered to be fulfilled.

Requirement R10 requires that the data collected by the solar module be stored so that it can be used later. The implementation of SD card storage in the solar module and

optional data transfer to the data platform guarantees that the collected data is stored, thus fulfilling this requirement.

Requirement R11 requires that the solar module withstand various weather conditions. As described in the implementation, the module's electronics are housed in a waterproof box, ensuring that the module is weatherproof. Therefore, this requirement is considered to be fulfilled.

Requirement R12 requires robustness and self-sufficient behavior. The solar module meets both sub-requirements. Robustness is ensured by various components and design decisions, which are explained in more detail in the implementation. And by connecting the solar panel to the battery at non-measurement intervals, the sub-requirement for self-sufficiency is also met as far as possible. This requirement is therefore also considered to be fulfilled.

Requirement R13 requires that the solar module itself is scalable. There are no limitations on the number of modules used to perform the scenarios mentioned above. Because of the ID of each module via the MAC address, a new identical solar module can be created at any time and initialized with the same program, integrating seamlessly into the data acquisition system. The scripts for analyzing the data could interpret the new data with minimal effort and evaluate additional modules. This requirement is therefore also considered to be fulfilled.

Requirement R14 requires that additional sensor data be collected in addition to the primary solar data. Special components are provided for this in the design and implementation, guaranteeing that the solar module can be expanded with additional sensors. This requirement is also considered to be fulfilled.

The final requirement R15 specifies that a single sensor system must be as inexpensive as possible. A detailed price list for the individual components can be found in the appendix to this thesis. The most considerable costs were for the solar panel and the battery used in the solar module. However, both components can be adjusted in size to minimize the price further, although this limits factors such as runtime. Furthermore, expensive controllers such as an MPPT controller were not used. The components were purchased from a German dealer, which ensures the quality of the individual components but is not the cheapest alternative. Care was therefore taken to keep the price as low as possible, but it could still be lower. This requirement is therefore only partially fulfilled.

Concerning research question Q2, this thesis has demonstrated that it is possible to design a solar module capable of recording precision solar data. The solar module developed in this thesis fulfilled most of the requirements and can be used as a basis for further work.

Regarding research question Q1, this thesis demonstrated a system capable of evaluating existing solar data sets using precision solar data. With the data set of the Solar Atlas Hamburg, it was shown that the large-scale data set has problems in non-optimal

environments. Furthermore, it was demonstrated that important detailed information is lost, meaning incorrect predictions cannot be ruled out.

8 Conclusion

This chapter begins with a summary of this thesis. After the summary a description of the significance of the results ist presented. The limitations that restricted the scope of this thesis are then discussed. At the end of the chapter, an outlook is given on how the research on solar data acquisition and evaluation of solar datasets could be continued.

8.1 Summary

This thesis uses a developed low-cost solar sensor module to determine the extent to which a large-scale solar data sets provide accurate data. To this end, a system for evaluation solar data sets and a solar module was designed. Various scenarios were carried out with the solar module to determine the extent to which the measured data differ from the data from the Solar Atlas of the city of Hamburg in order to make a statement about its accuracy.

The scenarios show that the solar atlas provide good data for estimating a good position for a solar panel. It was shown that good positions on different parts of a roof and different roofs provide the same data. It was also shown that the Solar Atlas can only make limited statements for suboptimal areas. Thus, measurement results in only suboptimal areas are highly variable and, therefore, unsuitable for deciding their actual performance. Further it was shown that the Solar Atlas has no information about local obstacles that can worsen the results. Thus, obstructions to solar radiation have a more substantial effect on the final power generation than the data from the Solar Atlas suggest. It has to be noted that the Solar Atlas does not contain any information about possible obstacles that would restrict the placement of a solar panel and is, therefore unsuitable for accurately determining a roof's solar potential for a specific position.

8.2 Implication of the Results

This thesis has shown that it is possible to create a cost-effective IoT solar sensor module that can collect comparable data for evaluation purposes. Further, the developed module can be adapted to capture any other sensor data, such as air quality, fine dust pollution, and light pollution, to create custom data sets for analysis or to evaluate existing data sets. Therefore, the solar module can make a concrete contribution to the further development of data-based urban infrastructures in the sense of a smart city.

Furthermore, the designed system can be used as a validation method for existing data sets. Large-scale analyses could serve as a basis, which are then enriched with the developed modules and their precision data. This way, the data can be updated when local conditions change or a higher resolution is necessary. If a new house is built that casts a shadow over the roofs, the data collected in solar data sets becomes unusable, and it is more suitable to update the data sets with precision data rather than complete renewing them. The developed modules can help keep the data up-to-date by placing them on the old roofs to collect new information. This System can also be applied to the other application areas with different sensors.

8.3 Limitations

The most significant limitation of this thesis is the temporal and spatial restriction of the measurements. This thesis uses data from a measurement period of just under three months as the basis for evaluation. This means that the different seasons cannot be represented, which could lead to data distortion. Furthermore, all measurements were carried out at one location so that there was a local bias in the data set obtained.

Another limitation is the solar module developed for data acquisition. Due to the decision not to implement an MPPT controller for cost reasons, a perfect comparison with conventional PV systems is impossible. Thus, deviations from the absolute measured values will always occur unless the solar modules are upgraded with such a controller. Furthermore, many quality-of-life features, such as the voltage divider for live battery performance monitoring, have not been completed due to time constraints.

The Solar Atlas as a dataset itself also represents a limitation. Since the raw data from the heat map does not contain specific values, it is impossible to compare absolute values with the data set. The additional data for the Solar Atlas already approximated values for some roofs in the city, and not all roofs have been recorded in the data set. Here, it would be helpful to consult additional solar data sets in order to compare and evaluate them with each other.

8.4 Outlook

First, it is possible to expand the scope of this thesis. For example, the measurement period can be extended to one year to capture average values for precise positions. In addition to the temporal dimension, the geographical dimension can also be scaled. Thus, the scope of data collection can be extended to even more roofs. If, for example, different roofs of other faculties are used, a broader sensor network can be created for the city of Hamburg which then again would diversify the data to avoid biases.

It would be interesting to evaluate other large-scale data sets in addition to the analysis from the Solar Atlas in the city of Hamburg. In addition, solar maps for rural areas, which

are usually based on satellite images, can be evaluated to assess their accuracy compared to the Solar Atlas. In this context, it could also be determined how different measurement methods, such as satellite images, laser detection, or precision measurement, can be compared with each other for solar data.

In addition to further evaluations, the module itself can be further developed. For example, additional sensors can be installed on the module, so that it could act as a complete sensor station for all possible data. Alternatively, the module could be equipped with motors to adjust its inclination to capture as much sunlight as possible to determine the best configuration for a precision point. Aspects such as energy optimization to guarantee a more extended, self-sufficient runtime or automatic calibration of the load for solar measurement (MPPT) can also be integrated to achieve even better results.

Meanwhile, the data collected by the modules could be used to design correction or prediction models for solar irradiation. In this way, it could provide the data needed for a digital representation of a roof to determine the best place for a solar installation in the virtual environment. If this is successful, the virtual model could be used to plan new buildings and include solar panels in the design phase. Alternatively, existing data sets can be efficiently supplemented with digital representations without carrying out any further local measurements.

Bibliography

[Ard25] Arduino. *Arduino*. https://docs.arduino.cc/hardware/uno-rev3/. [Accessed 07-04-2025]. 2025.

[Bri25] Gunnar Brink. "Die drei Säulen der Sonnenenergie: Photovoltaik, Photothermie und Concentrated Solar Power". In: *Energiewende 2.0: Innovationen für wirtschaftlichen Erfolg und eine lebenswerte Zukunft*. Wiesbaden: Springer Fachmedien Wiesbaden, 2025, pp. 93–136. ISBN: 978-3-658-46041-9. DOI: 10.1007/978-3-658-46041-9_5. URL: https://doi.org/10.1007/978-3-658-46041-9_5.

[Cam] Scott Campbell. *Basics of the I2C Communication Protocol — circuitbasics.com*. https://www.circuitbasics.com/basics-of-the-i2c-communication-protocol/. [Accessed 07-04-2025].

[Dha] Piyu Dhaker. *Introduction to SPI Interface*. https://www.analog.com/en/resources/analog-dialogue/articles/introduction-to-spi-interface.html. [Accessed 07-04-2025].

[Doz+23] Chikako Dozono et al. "Development of solar radiation measurement sensor with added value to promote wide-area solar power prediction technology". In: *Solar Compass* 7 (2023), p. 100054. ISSN: 2772-9400. DOI: https://doi.org/10.1016/j.solcom.2023.100054. URL: https://www.sciencedirect.com/science/article/pii/S277294002300022X.

[dwd25] dwd. *Wetter und Klima - Deutscher Wetterdienst - Startseite — dwd.de*. https://www.dwd.de/DE/Home/home_node.html. [Accessed 07-04-2025]. 2025.

[Ene25] Hamburger Energiewerte. *Solarrechner — solarrechner-hamburg.de*. https://www.solarrechner-hamburg.de. [Accessed 22-04-2025]. 2025.

[esp25] espressif. *espressif.com*. https://www.espressif.com/sites/default/files/documentation/esp32-wroom-32_datasheet_en.pdf. [Accessed 07-04-2025]. 2025.

[Fou25] OpenJS Foundation. *Express - Node.js web application framework — expressjs.com*. https://expressjs.com/. [Accessed 23-04-2025]. 2025.

[HAI21] Nazmul Hassan, Sakil Ahammed, and Abu Islam. "A Study of IoT based Real-Time Solar Power Remote Monitoring System". In: *The International Journal of Ambient Systems and Applications* 9 (June 2021), pp. 27–36. DOI: 10.5121/ijasa.2021.9204.

[Ham24] City Hamburg. *Hamburgs Solarrechner*. 2024. URL: https://www.hamburger-energiewerke.de/energieloesungen/stromversorgung.

[ibm25] ibm. *What is the Internet of Things (IoT)? | IBM — ibm.com*. https://www.ibm.com/think/topics/internet-of-things. [Accessed 11-04-2025]. 2025.

[Kat+18] Manish Katyarmal et al. "Solar power monitoring system using IoT". In: *Int Res J Eng Technol (IRJET)* 5.3 (2018), pp. 2395–0056.

[LGV25] LGV. *Geoportal Hamburg — geoportal-hamburg.de*. https://geoportal-hamburg.de/?lng=de. [Accessed 16-04-2025]. 2025.

[Mel+21] Gustavo Costa Gomes de Melo et al. "A Low-Cost IoT System for Real-Time Monitoring of Climatic Variables and Photovoltaic Generation for Smart Grid Application". In: *Sensors* 21.9 (2021). ISSN: 1424-8220. DOI: 10.3390/s21093293. URL: https://www.mdpi.com/1424-8220/21/9/3293.

[Mon25] Inc. MongoDB. *MongoDB: The World's Leading Modern Database — mongodb.com*. https://www.mongodb.com/. [Accessed 16-04-2025]. 2025.

[Nux16] Nuxt. *Nuxt: The Progressive Web Framework — nuxt.com*. https://nuxt.com/. [Accessed 16-04-2025]. 2016.

[Par25] Particle. *IoT and the Smart City: Examples, Applications, and Goals | Particle — particle.io*. https://www.particle.io/iot-guides-and-resources/smart-cities-iot/. [Accessed 11-04-2025]. 2025.

[R+23] Sivanand .R et al. "A Novel Approach to IoT-Based Solar Energy Measurement and Monitoring Model". In: 12 (July 2023), pp. 15777–15794. DOI: 10.48047/ecb/2023.12.si4.14122023.15/06/2023.

[ras25] raspberrypi. *Getting started - Raspberry Pi Documentation — raspberrypi.com*. https://www.raspberrypi.com/documentation/computers/getting-started.html. [Accessed 07-04-2025]. 2025.

[REC+15] Karen Rose, Scott Eldridge, Lyman Chapin, et al. "The internet of things: An overview". In: *The internet society (ISOC)* 80.15 (2015), pp. 1–53.

[Res25] Committed to Restoring America's Energy Dominance. *Solar Radiation Basics — energy.gov*. https://www.energy.gov/eere/solar/solar-radiation-basics. [Accessed 11-04-2025]. 2025.

[Roc+21] Álvaro B. da Rocha et al. "Development of a Real-Time Surface Solar Radiation Measurement System Based on the Internet of Things (IoT)". In: *Sensors* 21.11 (2021). ISSN: 1424-8220. DOI: 10.3390/s21113836. URL: https://www.mdpi.com/1424-8220/21/11/3836.

[RSY24] Challa Krishna Rao, Sarat Kumar Sahoo, and Franco Fernando Yanine. In: *Energy Harvesting and Systems* 11.1 (2024), p. 20230015. DOI: doi:10.1515/ehs-2023-0015. URL: https://doi.org/10.1515/ehs-2023-0015.

[San+22] Thiago Santos et al. "Design and validation of IoT measurement system for photovoltaic generation". In: *Ingenius* (July 2022), pp. 44–52. DOI: 10.17163/ings.n28.2022.04.

[Sis+18] Emiliano Sisinni et al. "Industrial Internet of Things: Challenges, Opportunities, and Directions". In: *IEEE Transactions on Industrial Informatics* 14.11 (2018), pp. 4724–4734. DOI: 10.1109/TII.2018.2852491.

[sol25] solcast. *Solar API and Weather Forecasting Tool | Solcast™ — solcast.com*. https://www.solcast.com/. [Accessed 07-04-2025]. 2025.

[SP13] Bidyadhar Subudhi and Raseswari Pradhan. "A Comparative Study on Maximum Power Point Tracking Techniques for Photovoltaic Power Systems". In: *IEEE Transactions on Sustainable Energy* 4.1 (2013), pp. 89–98. DOI: 10.1109/TSTE.2012.2202294.

[Sto+10] Tom Stoffel et al. *Concentrating solar power: best practices handbook for the collection and use of solar resource data (CSP)*. Tech. rep. National Renewable Energy Lab.(NREL), Golden, CO (United States), 2010.

[Tah+23] Muhammad Taha et al. "A Low-Cost IoT-Enabled Pyranometer; Based on the Peltier Element". In: *International Journal of Engineering Trends and Technology* 71 (Feb. 2023), pp. 334–340. DOI: 10.14445/22315381/IJETT-V71I2P235.

[tea12] The Matplotlib development team. *Matplotlib Visualization with Python - matplotlib.org*. https://matplotlib.org/. [Accessed 16-04-2025]. 2012.

[tea25] NumPy team. *NumPy — numpy.org*. https://numpy.org/. [Accessed 16-04-2025]. 2025.

[UHH25] UHH. *inf.uni-hamburg.de*. https://www.inf.uni-hamburg.de/service/location/lageplan.pdf. [Accessed 14-04-2025]. 2025.

[wet25] wetterkontor. *Deutscher Wetter Dienst - WetterKontor — wetterkontor.de*. https://www.wetterkontor.de/de/wetter/deutschland/rueckblick.asp. [Accessed 14-04-2025]. 2025.

[You14] Evan You. *Vue.js — vuejs.org*. https://vuejs.org/. [Accessed 16-04-2025]. 2014.

Appendix

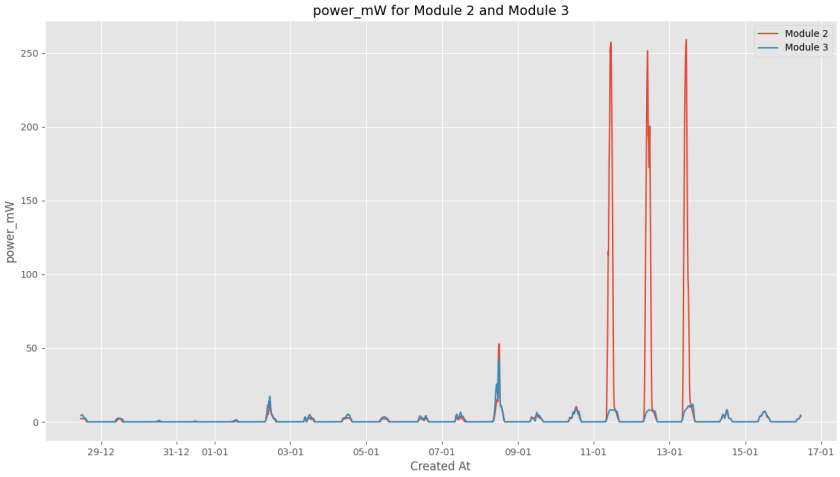

Figure 1: Power data evaluation selection between 29.12.24 to 16.01.25 of four solar modules of the first scenario.

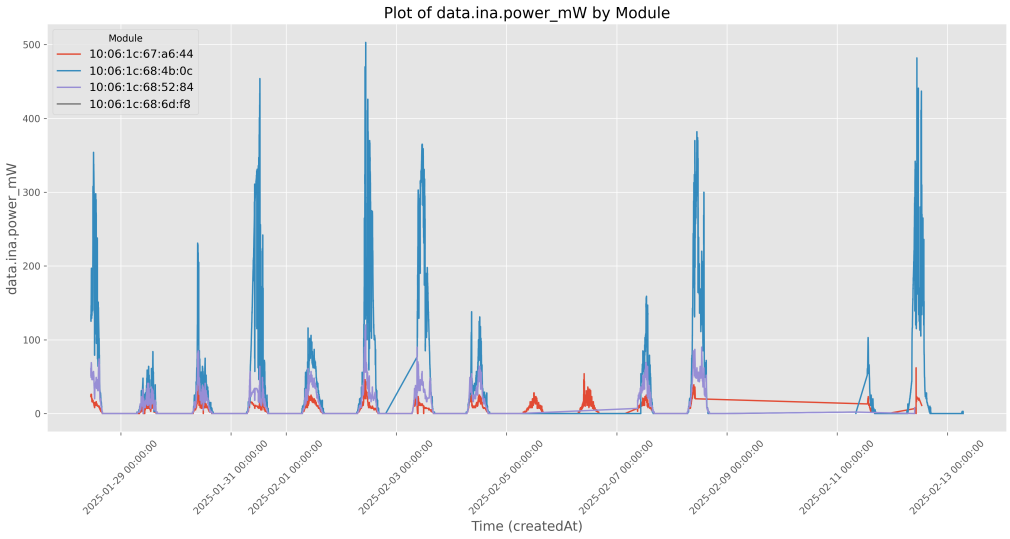

Figure 2: Power data evaluation selection between 29.01.25 to 13.02.25 of four solar modules of the second scenario.

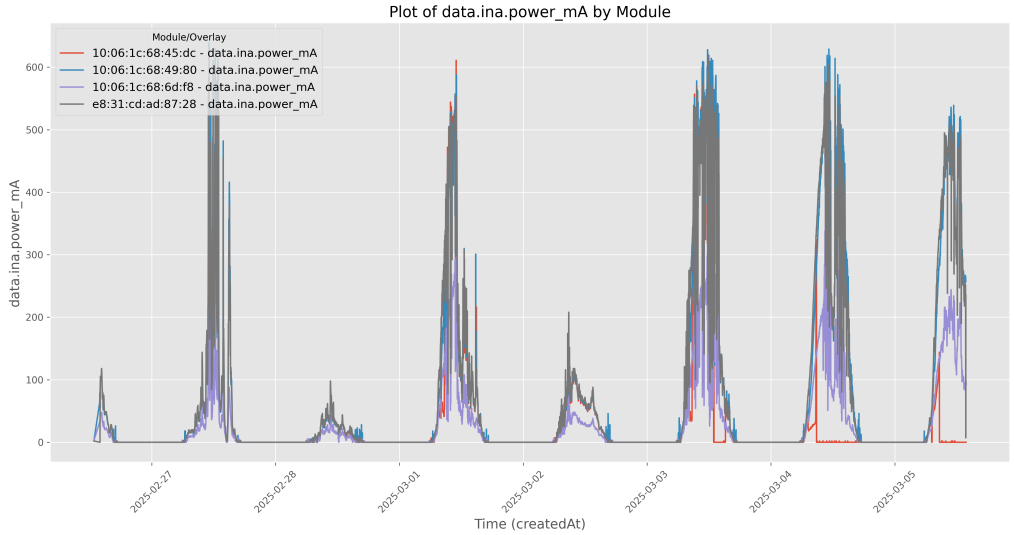

Figure 3: Power data evaluation selection between 27.02.25 to 05.03.25 of four solar modules of the third scenario.

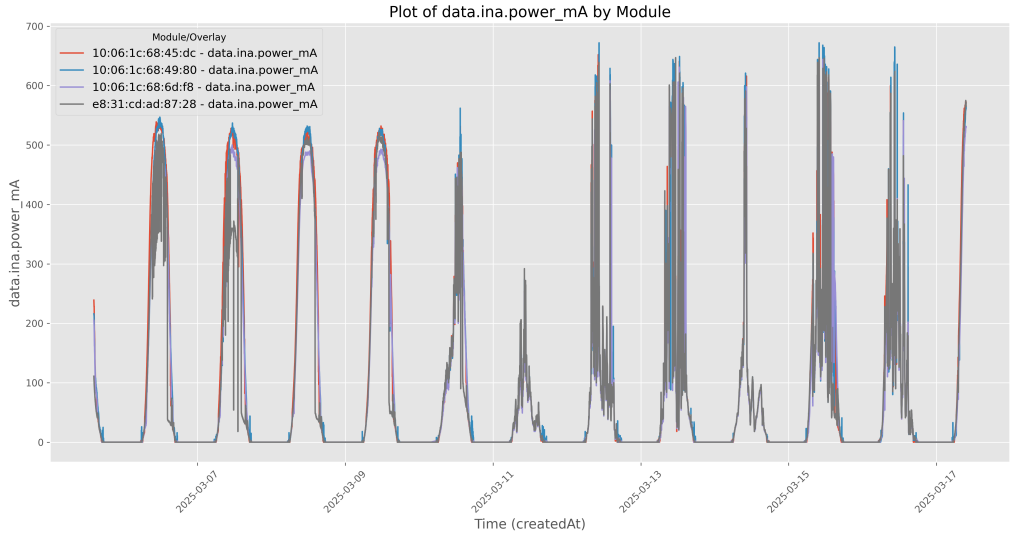

Figure 4: Power data evaluation selection between 06.03.25 to 17.03.25 of four solar modules of the fourth scenario.

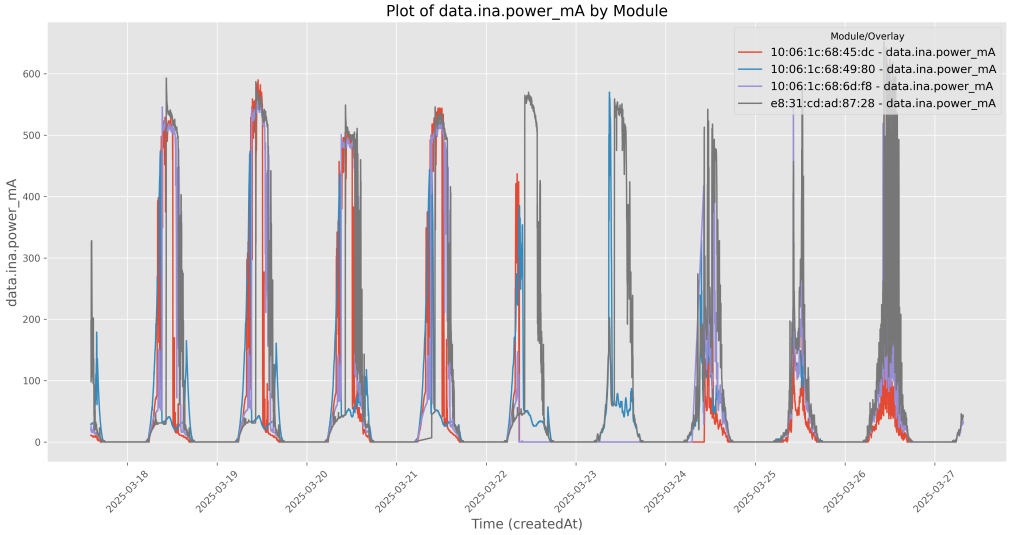

Figure 5: Power data evaluation selection between 18.03.25 to 27.03.25 of four solar modules of the fith scenario.

Component	**Count**	**Price (€)**	**Link**
Solar Panel	1	6,65	Shop
Akku 6000mAh	1	20,40	Shop
BMP180	1	4,40	Shop
Photodiode	1	1,25	Shop
Resistor 2W 8 Ohm	1	0,40	Shop
Resistor 2W 47 Ohm	1	0,40	Shop
SD Card Reader	1	2,40	Shop
SD Card	1	3,95	Shop
TC4056 Loading Board	1	1,85	Shop
INA219	1	4,70	Shop
Node MCU ESP32	1	9,10	Shop
Case	1	20,40	Shop
Step Up Module	1	4,99	Shop
Step Down Module	1	4,99	Shop
Relay	1	4,99	Shop
LED (Red, Green, Yellow)	3	-	-
Simple Resistors (3x 1K, 1x 10K)	4	-	-

Table 1: Component list for one solar module with prices and links

Eidesstattliche Versicherung

Hiermit versichere ich an Eides statt, dass ich die vorliegende Arbeit im Masterstudiengang Informatik selbstständig verfasst und keine anderen als die angegebenen Hilfsmittel – insbesondere keine im Quellenverzeichnis nicht benannten Internet-Quellen – benutzt habe. Alle Stellen, die wörtlich oder sinngemäß aus Veröffentlichungen entnommen wurden, sind als solche kenntlich gemacht. Ich versichere weiterhin, dass ich die Arbeit vorher nicht in einem anderen Prüfungsverfahren eingereicht habe. Sofern im Zuge der Erstellung der vorliegenden Abschlussarbeit generative Künstliche Intelligenz (gKI) basierte elektronische Hilfsmittel verwendet wurden, versichere ich, dass meine eigene Leistung im Vordergrund stand und dass eine vollständige Dokumentation aller verwendeten Hilfsmittel gemäß der Guten Wissenschaftlichen Praxis vorliegt. Ich trage die Verantwortung für eventuell durch die gKI generierte fehlerhafte oder verzerrte Inhalte, fehlerhafte Referenzen, Verstöße gegen das Datenschutz- und Urheberrecht oder Plagiate.

Hamburg, den _____ Unterschrift: _____

Veröffentlichung

Ich stimme der Einstellung der Arbeit in die Bibliothek des Fachbereichs Informatik zu.

Hamburg, den _____ Unterschrift: _____